Environmental Science & Technology
October 2015, Volume 49 Issue 19 Pages 11438-11448
http://dx.doi.org/10.1021/acs.est.5b01893
http://archimer.ifremer.fr/doc/00288/39884/

Evidencing the Impact of Coastal Contaminated Sediments on Mussels Through Pb Stable Isotopes Composition

Huy Dang Duc [1, 2], Schaefer Joerg [3], Brach-Papa Christophe [4], Lenoble Veronique [1], Durrieu Gael [1], Dutruch Lionel [3], Chiffoleau Jean-Francois [4], Gonzalez Jean-Louis [5], Blanc Gerard [3], Mullot Jean-Ulrich [6], Mounier Stephane [1], Garnier Cedric [1, *]

[1] Univ Toulon & Var, PROTEE, EA 3819, F-83957 La Garde, France.
[2] Trent Univ, Water Qual Ctr, Peterborough, ON K9J 7B8, Canada.
[3] Univ Bordeaux, UMR EPOC 5805, CS50023, F-33615 Pessac, France.
[4] IFREMER, Ctr Atlantique, LBCM, F-44311 Nantes, France.
[5] IFREMER, Ctr Mediterranee, LBCM, F-83507 La Seyne Sur Mer, France.
[6] LASEM Toulon, F-83800 Toulon, France.

* Corresponding author : Cédric Garnier, email address : cgarnier@univ-tln.fr

Abstract :

Heavily contaminated sediments are a serious concern for ecosystem quality, especially in coastal areas, where vulnerability is high due to intense anthropogenic pressure. Surface sediments (54 stations), 50 cm interface cores (five specific stations), river particles, coal and bulk Pb plate from past French Navy activities, seawater and mussels were collected in Toulon Bay (NW Mediterranean Sea). Lead content and Pb stable isotope composition have evidenced the direct impact of sediment pollution stock on both the water column quality and the living organisms, through the specific Pb isotopic signature in these considered compartments. The history of pollution events including past and present contaminant dispersion in Toulon Bay were also demonstrated by historical records of Pb content and Pb isotope ratios in sediment profiles. The sediment resuspension events, as simulated by batch experiments, could be a major factor contributing to the high Pb mobility in the considered ecosystem. A survey of Pb concentrations in surface seawater at 40 stations has revealed poor seawater quality, affecting both the dissolved fraction and suspended particles and points to marina/harbors as additional diffuse sources of dissolved Pb.

Graphical abstract

1. INTRODUCTION

Sources of trace metals in the environment are numerous, either natural or anthropogenic. The principal natural source of metals is crust weathering/erosion while a multitude of anthropogenic emissions occur in the environment (mining/smelting/metal manufacturing, fossil-fuel combustion, urban waste, sewage sludge, etc. [1]). Among these metals, Pb has been widely used for thousands of years (during Estruscan-Greek-Roman, medieval and modern periods [2]) due to its low melting point and corrosion resistance. Lead geochemical affinity is chalcophilic, resulting in the predominance of galena (PbS) as the main mineral of economic importance [1]. The four main Pb stable isotopes are ^{204}Pb, ^{206}Pb, ^{207}Pb, ^{208}Pb with average proportions of 1:17:15:37 [3,4]. Except ^{204}Pb which is not radiogenic, ^{206}Pb, ^{207}Pb, ^{208}Pb are the radioactive decay products of ^{238}U, ^{235}U and ^{232}Th, respectively. The Pb stable isotope ratios are widely used as a source tracking tool in environmental samples [2,5,6] as well as in organisms [7–9]. Among these organisms, bivalve molluscs and particularly mussels are consensually used as biological monitor organisms of coastal pollution due to their advantageous properties of sedentarity, large spatial distribution, easy sampling and pollutants bioaccumulation [7]. Several "mussel watch programs" (MWP) have been worldwide active for decades (France: RNO/ROCCH [8,10], Spain [7], USA [11], ect.). The most important Pb sources assessed by Pb isotope signatures are coal combustion, leaded gasoline, metal smelting, battery factories, sewage sludge and waste incineration [1,2]. Another recent source of metals, including Pb, could be their growing use in antifouling paints [12,13]. In coastal ecosystems, sediments accumulate settling contaminated particles, providing historical archives of pollution [14]. Such sediments could also be a serious concern for the ecosystem quality [15] due to numerous biogeochemical processes within sediments and at the sediment/water interface (SWI) [16–19]. However, it remains a complex issue to interlink sediment contamination with the degradation of water quality and the living organisms' exposure to pollutants, as a prerequisite for an adapted environmental policy.

Toulon Bay (NW Mediterranean sea) sediments are extremely contaminated by a multitude of metals/metalloids/organo-metallics [17,20–22] and organic contaminants (unpublished data). Such status originated both from historic (bombardments, warship scuttling and -raising during and after the 2nd World War [21]) and more recent activities (main French Navy harbor, nautical traffic, release of sewage from the Toulon urban area, industries, tourism…), coupled with its

characteristics (semi-closed area, low tidal amplitude, long water/particle residence time [23]). Analysing data from the MWP, Andral et al. [24] have observed that Toulon Bay mussels had, by far, the highest Pb concentrations over 1800 km of the French Mediterranean coast (~5.4 µg g^{-1}, dry weight, in comparison to an average value of 1.0 (n = 91)), together with huge anomalies in other pollutants (DDT, CB153, Hg, …). Trace metals concentrations monitoring both in water and mussel samples from Toulon Bay has shown clear co-variations [25], even if the origins of high Pb and Hg levels still remain unclear. All these observations, associated with the presence of aquaculture activities (fish and mussel farming) inside the bay, raise numerous questions about the potential mobility of such pollutants and further risks for the surrounding environment, making this site a model environment to study such processes which also act in many other areas.

The present study reports on Pb levels and isotope signatures in sediments, seawater and mussels of the Toulon Bay, focussing on its origins and pathways between these compartments. The objective was to investigate whether the historical sediment Pb pollution together with resuspension cycles may explain the exceptionally high Pb contamination in both farmed and wild mussels. Lead concentrations and isotope ratios were measured in (i) total and 1 M-HCl extracts of surface sediments (0-5 cm) and 50-cm interface sediment cores, (ii) farmed mussels from the RNO/ROCCH sample bank covering the 1979-2012 period and wild mussels collected in the most contaminated area, (iii) particles issued from small tributaries and hazardous material (coal block and battleship's bulk Pb plate from French Navy) and (iv) surface seawater samples around the Toulon Bay. Finally, resuspension experiments with surface/deep sediments covering a wide range of Pb contamination levels aimed at studying Pb behaviour and remobilisation kinetics.

2. MATERIALS AND METHODS

2.1. Study site and sampling

The Toulon Bay hosts a large urban area on the French NW Mediterranean coast where various anthropogenic activities (Navy/civil harbours, aquaculture, urban sewage release, industries...) have resulted in severe multi-contamination of the ecosystem, especially in sediments [17,20–22]. The bay is divided by a seawall (N–S straight line, Fig. 1) in two non-

equivalent parts (Small and Large Bay). Two urban river outlets (Las and Eygoutier Rivers) represent the main freshwater inputs to the bay, located on the north shore, whereas the main anthropogenic activities cover large areas around the Toulon Bay (Fig. 1). In these two tributaries (Las and Eygoutier Rivers), particle traps [26,27] were installed by IRSN (Radioprotection and Nuclear Safety Institute) to assess the terrestrial contribution to the coastal system. Five particles samples were collected in each tributary using 2 weeks collection periods from October 2012 and May 2013, mostly during rain events [28].

The studied sediments were collected at 54 stations covering the whole bay (Fig. 1) using an interface corer (10-cm diameter and 1-m long Plexiglass® tube) with the support of the French Navy (boats, materials, divers), as detailed elsewhere [16,18,20,28]. Briefly, for each site, duplicate cores were sliced for surface sediments (0-5 cm) and slices were pooled, homogenized in HDPE 1-L bottles and deep-frozen (-18°C). Moreover, interface sediment cores (~50 cm) were sampled at five specific stations (MIS, 3B, 12, 15 and 23, Fig. 1). Only cores with well-preserved SWI were analysed. The stations MIS and 3B are located in the Navy area, the station 12 is close to a former Navy submarine base and the station 15 is in the aquaculture area. Finally, the station 23 is situated in the Large Bay, in front of the Eygoutier River outlet. The interface cores were sliced with 2 cm resolution under inert atmosphere (N_2). Slices were then centrifuged (4000 rpm, 15 min, Sigma 3-18K). Porewater was recovered in a glove-box by filtration (0.2-µm on-line syringe filters, cellulose nitrate, Sartorius) and stored in the adapted vessels, more details in Dang et al. [17]. The solid fraction was deep-frozen in HDPE bottles, freeze-dried, 2-mm sieved and kept deep-frozen (-18°C) until analysis.

To evaluate the surface (0.5 m) distribution of Pb concentrations in the water column of Toulon Bay, water samples were collected at 40 stations covering the whole bay in early summer (June 24th, 2013) and winter (February 17th, 2014). For each station, raw (unfiltered) and on-field filtered (0.2 µm cellulose nitrate syringe filter, Sartorius) seawater samples were stored in 125-mL FEP bottles (Nalgene), previously acid-cleaned (10% HNO_3, pro analysis), thoroughly rinsed with mQ water (18.2 MΩ, Millipore) and acid-conditioned (0.1% HNO_3, s.p., Merck) before being rinsed with raw/filtered water from the site. Raw and filtered samples were then acidified (0.2%, HNO_3, s.p., Merck) and digested for 24h under UV irradiation (150W [29]) to assess the dissolved and total acid-leachable (hereafter considered as "total") concentrations, respectively. Additional surface water (0.5 m) was sampled in 2-L

HDPE pre-cleaned bottles at 6 stations the 21st of October 2013 (Fig. 1) to analyse Pb isotopic signature.

Farmed mussels (35-65 mm, *Mytilus galloprovincialis*) were sampled in the aquaculture area close to the station 15 within the framework of the RNO/ROCCH program since 1979 (seasonally until 2002 and twice a year (February and November) since 2003). Wild mussels were sampled in 2014 at station MIS, 12 and close to Milhaud dock (Fig. 1). The mussels (at least 50) were depurated for 24 h in a polyethylene aquarium filled with filtered seawater from the station. The soft tissues were separated from shells, pooled, freeze-dried and deep-frozen (-20°C).

During the dredging operations started in 2013 in the area around the station 3B, huge quantity of coal blocks were discovered in sediments. The inscribed signs ("Anzin, 1912", Fig. S1) illustrated its origin (North of France) and the period. An aliquot was crushed and burned out at 550 °C. The powder was digested on a hot plate with HCl/HNO_3 solution at 110 °C until complete acid evaporation before dilution with HNO_3 (s.p, Merck) for Pb concentration and Pb isotopes analysis.

Finally, a bulk Pb plate (~0.5 m², Fig. S1) originating from the French Navy battleship "Magenta", sunk in 1876 in the North of Toulon Bay, was collected by Navy divers in April 2015 from the battleship's beaching area (at 15 m depth, near the Toulon Navy harbour entrance). Aliquots were cut up, and then submitted to the same protocol as coal powder for Pb isotope analysis.

2.2. Sediment and mussel samples analysis

Pseudo-total element contents in sediments and tributaries particles were measured after aqua regia/microwave digestion according to a previously described protocol [21,29] and validated using PACS-2 certified materials (National Research Council of Canada; accuracy between 0.9 and 7% according to the considered element [21,29]. HCl extraction (1M HCl, s.p. Merck) was performed to assess the potential bioavailability and mobility of major and trace elements [17,29,31].

Farmed mussels (dried powder of *Mytilus galloprovincialis*) were taken from the French national mussel watch programme sample bank (RNO/ROCCH; IFREMER). Aliquots (150 – 200 mg) were digested with 8 mL of HNO_3 (ultrapure), in a microwave oven (MARS-5, CEM

161 Corporation), equipped with a carousel holding 12 Teflon vessels and under temperature and
162 pressure control. After cooling, digests were diluted to 50 mL with mQ water.
163 Lead concentrations in semi-total and 1M-HCl extracts of sediments (108 from surface
164 cartography, 184 from interface cores, 10 tributary particles) were analyzed by High
165 Resolution Inductively Coupled Plasma Mass Spectrometer at RBI-Zagreb laboratory (HR
166 ICP-MS, Element 2, Thermo Finnigan, more details in Lenoble et al. [32]).
167 Stable Pb isotopes (^{206}Pb, ^{207}Pb, ^{208}Pb) were measured by quadrupole ICP-MS on (1) a
168 representative set of sediments samples (34 surface sediments, 70 from interface cores (53
169 semi-total and 17 1M-HCl extracts), 10 tributary particles) at EPOC laboratory-Bordeaux
170 (XSeries 2, ThermoScientific, more details are presented by Petit et al. [33]); and on (2) mussels
171 extracts at LBCP-IFREMER laboratory (Element X series, Thermo Electron Corporation).
172 Mass bias and instrumental drift were corrected with a standard bracketing method by
173 analyzing NIST SRM-981 standard reference material. The ^{207}Pb/^{206}Pb and ^{208}Pb/^{206}Pb
174 internal relative standard deviation were in the range of 0.16-0.24% (n = 192) and 0.10-0.16%
175 (n = 10) for sediments and mussels analysis, respectively.
176
177 2.3. Seawater sample analysis
178 Total and dissolved Pb concentrations in seawater samples were determined by Differential
179 Pulse Anodic Stripping Voltammetry (DPASV). More details on instruments and analytical
180 procedure are described elsewhere [34]. Iron and Mn concentrations in water samples from
181 sediment resuspension experiments (see part 2.4) were measured by HR ICP-MS (RBI
182 laboratory).
183 Seawater samples for Pb isotopes analysis were filtered (0.45 µm, polycarbonate, Nucleopore)
184 under nitrogen pressure. Filtrates were acidified (0.1% HNO_3 s.p.) and stored in polyethylene
185 double-bags protected bottles. Quantitative Pb extraction from the seawater matrix was
186 performed by dithiocarbamate chelation, extraction into an immiscible organic solution and
187 back-extraction with diluted HNO_3 following an adapted protocol of Danielsson et al. [35], as
188 described by Chiffoleau et al. [36]. In brief, a sample aliquot (400 - 500 g) was buffered to pH
189 5.5 with ammonium acetate (s.p.) solution. APDC/DDDC chelating solution was then added
190 and shaken to homogenize. Freon was added next and vigorously shaken. After phase
191 separation, the Freon phase was carefully collected. This Freon extraction step was repeated

192 twice. The collected organic phase was then treated with 0.5 mL HNO_3 (s.p.) and 2 mL mQ
193 water to degrade the dithiocarbamate chelates. After vigorous shaking and phase separation,
194 the aqueous phase was collected. 1 mL of the extract was diluted to 5 mL with mQ water.
195 Stable Pb isotope ratios were measured according to the same procedure as mussel samples.
196 In addition, ICP measurements of the procedural blanks was verified to reach values around
197 500 cps (^{208}Pb), when samples were adjusted (by dilution) to ~100 000 cps. The blank signal
198 only accounted for less than 1% of the sample signal.
199
200 2.4. Sediment resuspension experiments
201 In order to assess the potential of Pb mobilization during sediment resuspension events (e.g.
202 storm, boat traffic, dredging …), laboratory experiments were performed using sediments
203 from various sites presenting a large range of contamination. Sediment cores from stations
204 MIS, 3B, 12 and 15 were sliced under N_2 conditions, and aliquots of surface/suboxic (0-2 cm,
205 stations MIS, 3B, 12 and 15) and deep/anoxic (20-22 and 30-32 cm for stations 3B and MIS,
206 respectively) sediments were kept under inert atmosphere until the start of resuspension
207 experiments. To ensure close replication of natural conditions no pre-treatment (e.g. seawater
208 filtering or UF irradiation, autoclaving, poisoning, …) of the sediment or seawater was
209 performed. However, more detailed experimentation would be necessary to delineate the roles
210 of the various components (e.g., microbes, DOM, minerals, ...).
211 The solid/liquid (S/L) ratio was setup to ~1 g L^{-1} (expressed in dry weight), a value close to
212 in-situ levels of SPM measured during surface sediment reworking (personal data). Sediment
213 aliquots were then transferred into pre-cleaned 2 L FEP bottles (Nalgene), and filled with the
214 corresponding unfiltered surface (0.5 m below the surface) seawater from each sampling
215 station. FEP bottles were then immediately submitted to overhead shaking (15 rpm, Heidolph
216 Reax 20) for 2 weeks. After 10 different contact times (5, 15, 30 min, 1, 3, 7 h, 1, 2 days and
217 1, 2 weeks), agitation was stopped for few minutes to allow particles settling, then 50 mL
218 aliquots (or 250 mL at 1 h, 7 h and 2 w) were sampled from the surface of the supernatant
219 using pre-cleaned syringes and FEP tube, immediately filtered through 0.45 µm filters
220 (hydrophilic PTFE, Millex LCR, Millipore), stored in 60 mL FEP bottles, acidified (0.2%
221 HNO_3, s.p., Merck) and UV-digested as previously described, before dissolved Pb, Mn, Fe
222 concentrations measurement. Lead isotope analysis was performed on aliquots collected at 0,

1, 7 h and 2 weeks of contact time following the procedure described in section 2.3. To minimize S/L ratio variations, 50 mL (or 250 mL at 1 and 7 h) of unfiltered seawater were injected at each sampling time. To maintain stable oxic conditions (i.e. as encountered in the bay water column during sediment resuspension due to dredging or boat traffic), FEP bottles were opened every day for a few minutes during the whole experiment. Parallel resuspension batches were performed in separate HDPE bottles to monitor the daily variations of physico-chemical parameters (T, pH, Eh, dissolved O_2) using multi-probes (Hach Lange).

3. RESULTS AND DISCUSSION

3.1. Lead distribution and isotopic composition in sediments

Previous studies [17,20–22,29] have evidenced the huge stock of contaminants (inorganic, organometallic and organic) in the northern Small bay and non-negligible levels in the rest of the bay (Fig. 1). Within the broad Pb content range (15-470 µg g^{-1}), the $^{206}Pb/^{207}Pb$ ratio variation was unexpectedly low (1.156-1.180), with an average value of 1.168±0.005 (n = 34). The lowest $^{206}Pb/^{207}Pb$ ratios (1.156-1.167) occurred in the most contaminated zones (Navy area, former shipyard, La Seyne s/Mer harbour) and the highest $^{206}Pb/^{207}Pb$ ratios (~1.174-1.180) occurred in the less contaminated area. Similar results were obtained using $^{206}Pb/^{208}Pb$, with an average value and variation range of 0.475±0.001 (n = 34) and 0.474-0.478, respectively (Table 1). The Pb 1M-HCl extractability was similar, close to 64±6 % (n=50), for all the stations [29] and the Pb isotopic composition of 1M-HCl extracts was identical to that of Pb in total digestions (n=10).

Total Pb, HCl-extracted Pb content and Pb stable isotopes depth profiles from 5 stations (MIS, 3B, 12, 15 and 23) are shown in Fig. 2 and A.1 and compared to previously published Pb depth profiles from stations 3B, 12 and 15 [21,29]. At stations MIS and 3B, the observed Pb contents were extremely high all down the cores (380-1300 and 201±29 µg g^{-1}, respectively) with the majority in the HCl-extracted fraction (~80±8 % at station 3B). Such deep extension of Pb contamination, corresponding to an incoherent period of time if considering a stable sedimentation rate estimated around 0.2 cm yr^{-1} for the whole bay[21] are probably the consequence of sediment disturbance due to past (raising of scuttled warships) and present (e.g. harbour extension) activities. In these sediments, the $^{206}Pb/^{207}Pb$ and $^{206}Pb/^{208}Pb$ ratios,

either in the total or the HCl-extracted fraction, were stable and close to the values encountered in surface sediments (Fig. 2, Fig. S2, Table 1). Both high Pb contamination and specific Pb isotope ratios in different parts of the Toulon Bay support the idea that the Pb sedimentary contamination at the scale of the bay mainly originates from a main source, situated in the military area, mainly linked to past events (2nd World War) and resulting from the multiplicity of Pb uses by Navy (e.g. weapons, batteries, hull protection, weights, antifouling, explosive, …). Hereafter, the Pb stock with $^{206}Pb/^{207}Pb$ and $^{206}Pb/^{208}Pb$ values (1.165±0.004 and 0.475±0.001 (n = 14), respectively) is called $^{anthropogenic}Pb$ (Table 1).

At station 12, a strong contamination peak occurred for many pollutants (Ag, Cd, Cu, Hg, Pb, Zn, Sn, ΣBT) at -11 cm [20,21,29] (Fig. 2). Deeper, smaller peaks at -25, -40 and -50 cm were hypothetically attributed to a partial burying of contaminated sediment due to nautical/harbour activities [21]. The present Pb isotope signatures undoubtedly confirm these hypotheses: the main multi-contamination peak has the typical $^{anthropogenic}Pb$ signature, similar to that of deeper peaks. Between these small peaks, the non-negligible Pb burdens (70-110 µg g^{-1}, Fig. 2) in deeper sediment layers show slightly higher $^{206}Pb/^{207}Pb$ and $^{206}Pb/^{208}Pb$ ratios, i.e. values closer to the natural signature ($^{natural}Pb$, 1.195±0.014 and 0.483±0.003 (n = 16), respectively, Table 1 and A.1). Concerning the HCl-extracted fraction, a similar $^{206}Pb/^{207}Pb$ ratio and a slightly lower $^{206}Pb/^{208}Pb$ ratio were recorded in surface sediments compared to deep sediments. In parallel, the HCl-extracted Pb percentage increased from ~22±6 % (n=7) in the surface sediments to ~45±3 % (n= 18) below -15 cm.

Stations 15 and 23 showed similar depth profiles of Pb content and isotope ratios (Fig. 2 and Fig. S2). Surface layers (0-15 cm) had quasi-constant Pb contents (92±6.9 and 65±5.4 µg g^{-1}, respectively), along with the $^{anthropogenic}Pb$ signature. Deeper, both cores displayed decreasing Pb concentrations along with increasing $^{206}Pb/^{207}Pb$ and $^{206}Pb/^{208}Pb$ ratios, reaching the local background of Toulon Bay (~13.6 µg g^{-1}, [21]) and typical signature of $^{natural}Pb$. Contrarily to the station 12, the Pb acid extractability was significantly higher for the surface sediments (~76±4 %). A similar $^{206}Pb/^{207}Pb$ ratio and a slightly higher $^{206}Pb/^{208}Pb$ ratio were observed.

The accumulation of $^{anthropogenic}Pb$ in the first 10-12 cm (corresponding to the past 50-70 years [21]) at stations 12, 15 and 23 suggests a main common historical pollution event. The dispersion of these Pb contaminated particles (and associated pollutants [20–22]) is probably still a major pollution source for the more distal parts of the bay. This ongoing pollution spreading

is most probably activated by natural (storm, waves, etc.) or anthropogenic (large boat traffic, harbour activities, etc.) resuspension of the contaminated sediments in the north part of Toulon Bay, followed by particles transport-settling-resuspension processes driven by bottom water hydrodynamics [23,37].

3.2. Pb content and source in mussels

The Pb contents ranged from 2.2 to 18.7 μg g^{-1} in farmed mussels (1979-2012) and from 14.7 to 27.8 μg g^{-1} in wild mussels (Fig. 3). These values were much higher than those measured in the same species along the French Mediterranean coast (~1.0 μg g^{-1} [24]), Italian coast (0.07 to 4.2 μg g^{-1} [38]) or American coast (low: 0-3 μg_{Pb} g^{-1}; medium: 4-6 μg_{Pb} g^{-1}; high: 7-13 μg_{Pb} g^{-1} [11]). Except the 1985-1991 period, it appeared that Pb concentrations in mussels were systematically higher in winter/spring period than summer/fall due to biological dilution during reproduction cycles [8]. Apart from such intra-annual variation, the long-term Pb accumulation in mussels seemed to slightly decrease, inversely to the $^{206}Pb/^{207}Pb$ ratio which tended to increase, still being in the range of $^{anthropogenic}Pb$ values (Fig. 3). A similar trend was observed for mussels (*Mytilus edulis*) from other sites along the French Atlantic coast [8]. The $^{206}Pb/^{207}Pb$ ratio in Toulon Bay mussels (~1.163±0.004, n = 31) was close to that reported in the literature (~1.167 in the Norman-Breton Gulf, ~1.161 in the Seine Estuary [8]). Labonne et al. [39] have evidenced 3 isotopic domains in Thau Lagoon mussels, corresponding to 3 spatial areas: sea ($^{206}Pb/^{207}Pb$ ~1.170-1.176), harbour ($^{206}Pb/^{207}Pb$ ~ 1.162-1.169) and coastal runoff/chemical-impacted zones ($^{206}Pb/^{207}Pb$ ~1.158-1.161). This last specific signature corresponded to the $^{anthropogenic}Pb$ signal measured in both Toulon Bay sediments and mussels, suggesting that mussels are exposed to similar Pb source.

The observed very high levels of $^{anthropogenic}Pb$ in mussels, which equalled or even exceeded the average (~1.4±0.1 μg g^{-1}) and the highest levels (~8.3 μg g^{-1}) recorded on a large scale survey of the Western Mediterranean coastal waters [40], could be of serious concern. The observed Pb levels often surpassed the French limit for mussel consumption (7.5 μg g^{-1} [41,42]). The common evolution of Pb isotope signatures encountered in both sediments and mussels from Toulon Bay clearly suggests a close link between these compartments.

3.3. Tracing Pb sources and Pb remobilization mechanisms

316 Different source-specific Pb isotope signatures from the literature were plotted to define the
317 domains of variations for the main Pb sources (Table S1; Fig. S3) and the results obtained for
318 Toulon Bay sediments, tributary river particles, coal, battleship's Pb plate, mussels and
319 surface seawater were then compared to these various sources (Fig. 4). The deeper layers at
320 stations 12, 15 and 23 showed ^{natural}Pb signatures. All the other sediment samples had typical
321 ^{anthropogenic}Pb signatures. When compared to literature data (Fig. 4A), this quite characteristic
322 signature (^{206}Pb/^{207}Pb ~ 1.166±0.003 and ^{206}Pb/^{208}Pb ~ 0.475±0.001, n = 56, Table 1) is
323 common to the domains of industries (metal refinery), European coal and urban wastes. Such
324 Pb isotopic ratios were also close to those of ore deposits in Italia (^{206}Pb/^{207}Pb ~ 1.161;
325 ^{206}Pb/^{208}Pb ~ 0.474) and Spain (^{206}Pb/^{207}Pb ~ 1.167; ^{206}Pb/^{208}Pb ~ 0.472) [4]. The "Anzin" coal
326 (total Pb content ~300 µg g^{-1}) presented a Pb isotope signature significantly different from
327 ^{anthropogenic}Pb, either as bulk or ash, probably contributing only slightly to the overall Pb
328 contamination.
329 As the ^{anthropogenic}Pb signature appeared to significantly differ from that of ^{natural}Pb, it was
330 possible to estimate the contribution of the Pb contamination in sediments, using a binary
331 mixing model [43], according to the following equation:
332

$$X_i = \frac{^{i}\left(^{206}Pb/^{207}Pb\right) - {}^{natural}\left(^{206}Pb/^{207}Pb\right)}{{}^{anthropogenic}\left(^{206}Pb/^{207}Pb\right) - {}^{natural}\left(^{206}Pb/^{207}Pb\right)}$$

333 (Eq. 1)
334 where X_i is the percentage contribution of ^{anthropogenic}Pb source in sample i; ^{i}(^{206}Pb/^{207}Pb),
335 ^{anthropogenic}(^{206}Pb/^{207}Pb) and ^{natural}(^{206}Pb/^{207}Pb) are the isotopic signatures in the sample i and the
336 main identified Pb sources in Toulon Bay, respectively.
337 The spatial distribution of X_i values in surface sediments of the Toulon Bay (Fig. S5) clearly
338 showed the generally dominant contribution of the ^{anthropogenic}Pb source, being at least of 43%
339 in the Large Bay and >99% in the Small Bay.
340 The Pb concentrations in particles transported by the Las and Eygoutier Rivers ranged from 8-
341 40 and 24-123 µg g^{-1} (n=10), respectively. In the most contaminated particles, the Pb isotope
342 signature was close to that of ^{anthropogenic}Pb. However, the regression line's slope of ^{206}Pb/^{208}Pb
343 over ^{206}Pb/^{207}Pb ratio in particles was higher than that obtained for sediments (Fig. 4A). This
344 observation, in addition to the lower Pb content in Las particles compared to the Small Bay

sediments suggests that present river-borne continental inputs only partially contribute to the poor quality of Toulon Bay sediments, mainly influenced by past nautical activities. Indeed, Pb isotope signature of the "Magenta" French Navy battleship's Pb plate was close to that of ^{anthropogenic}Pb (Fig. 4A). Even if the contamination of Toulon bay sediments cannot be induced by bulk Pb originating from a unique battleship sunk in the 19th century, it illustrates the signature of the Pb which was used by the French Navy and had mostly contributed to the excessive contamination of the bay during the 2nd World War.

The slight increase in $^{206}Pb/^{207}Pb$ ratios in farmed mussels to reach ^{anthropogenic}Pb value since the 1990s, (Fig. 3) could partly reflect the withdrawal of the contribution of leaded gasoline (^{gasoline}Pb, $^{206}Pb/^{207}Pb = 1.084\pm0.010$ and $^{206}Pb/^{208}Pb = 0.458\pm0.002$ (n = 9) [43], Table 1, A.1) due to the progressive substitution of leaded gasoline in France since the 1990s and its total prohibition in 2000. However, the historical record of Pb isotope ratios in farmed mussels suggests that the contribution (from atmosphere and tributaries inputs) of ^{gasoline}Pb (compared to ^{anthropogenic}Pb using a binary mixing model equation similar to Eq.1) has decreased from 18% in 1980s to an extremely low level (<0.5%) since 2004. Accordingly, the observed Pb isotope signals provided clear evidence that the local ^{anthropogenic}Pb contamination has always been greatly dominant, even during the period of maximum leaded gasoline use. The extremely high Pb content (up to 28.8 µg g^{-1}) and ^{anthropogenic}Pb isotopic composition (Fig. 3) in wild mussels in the most polluted area highlights the strong exposure and response of filter feeders to sediment contamination. However, the exact pathway between contaminated sediments and mussels did not become obvious, considering the various mechanisms controlling metal absorption by mussels and other bivalves, which can involve (i) direct assimilation of dissolved metals [9,44,45], (ii) ingestion of metal-contaminated phytoplankton [46], (iii) ingestion of contaminated particles (e.g. sediments) [47] or (iv) mixed mechanisms [48–50].

The two mapping campaigns provided a view on the spatial distribution of dissolved Pb levels in surface water of the Toulon Bay. The dissolved Pb concentrations measured in Winter 2014 were up to 29 times greater than those in unpolluted Mediterranean waters (~0.085 nM [51]) and confirmed previous observations [25,52] showing that Toulon Bay water is strongly contaminated by Pb (Fig. 5A). The highest Pb concentrations in surface water occurred in harbour/marina areas (Fig. 5A), coinciding with higher Pb contents in sediments (Fig. 1). Results obtained in summer 2013 (data not shown) displayed similar trends. The total vs. dissolved Pb

concentrations (slope = 1.97, r^2 = 0.86, n = 80, Fig. S6) showed an equi-repartition of this trace metal between dissolved and particulate fractions (K_d value ~5×10^5 L kg^{-1}, considering an average SPM concentration of 2 mg L^{-1}), confirming its high affinity for particles [53,54]. The 6 surface seawater samples collected at various places of the Toulon Bay (Fig. 1) to assess seawater Pb isotopic signature covered a representative range of concentrations (0.2-1.8 nM). Their corresponding Pb isotopic signature ($^{206}Pb/^{207}Pb$ ~ 1.166±0.002 and $^{206}Pb/^{208}Pb$ ~ 0.475±0.001, n = 6) appeared to fall exactly in that of $^{anthropogenic}Pb$ (Fig. 4B). Even if these results did not enable the preferred mussel pathway of Pb assimilation from dissolved and particulate fractions to be distinguished, common spatial distribution and isotope signals strongly support the existence of a direct link between the Pb contamination of Toulon Bay's water column and contaminated sediments, which could originate both from trace metals diffusive flux through the SWI [29,55] or remobilisation during sediment resuspension [56].

The obtained kinetics of Pb remobilisation during simulated resuspension of different Toulon Bay sediments reveal both common points and sediment-specific responses (Fig. 5B). As expected, the measured physico-chemical parameters (pH, Eh, O_2...) remained stable all along the experiments (data not shown), maintaining oxic conditions, even if a slight acidification was noticeable after a few days (e.g. surface sediment from stations 3B and MIS, Fig. S4). Confirming previous results, Pb concentrations initially measured at each site (time of 0.01 h, Fig. 5B) reflected the contamination pattern in Toulon Bay's waters as observed during the mapping campaign, following a South-North gradient from 0.40 to 1.65 nM (station 15 and MIS, respectively). From this initial status, resuspension of surface/suboxic sediments (0-2 cm layer from the 4 stations, characterized by Eh values ranging from -105 to –2 $mV_{/ENH}$) systematically induced significant Pb remobilisation, reaching maximal values after a few hours of contact time, probably due to desorption processes [57]. The Pb release from sediment increased the initial Pb concentration by up to 5-13 fold, reaching levels as high as 9.9 nM (i.e. 120 fold the level in unpolluted Mediterranean waters [51]), although the maximal proportion of mobilized Pb from the solid fraction remained low (0.15 to 0.5%, n = 6). Deep sediment (20-22 cm) from station 3B showed quasi-similar behaviour as surface sediments from the same site (Fig. 5B). As previously discussed (section 3.1.), sediments from this area were submitted to reworking and partial mixing, resulting in a burying of the contamination (Fig. S2), and modifying the diagenesis processes, with a sulfidic layer appearing as deep as -

30 cm [17]. For all these sediments, the rapid Pb remobilisation was systematically followed by Pb removal after days to weeks of contact time (Fig. 5B), a behaviour already observed elsewhere [13]. Contrarily, resuspension of the deep/anoxic sediment layer (30-32 cm) from station MIS induced a first rapid removal until 1h of contact time, followed by a continuous remobilisation reaching the highest recorded Pb level (22 nM). This succession of Pb remobilisation/removal steps reflects adsorption/desorption and/or co-precipitation/dissolution processes at different scales, which can partly be explained by the variations of the other parameters. For example, the Fig. S4 represents the temporal variations of pH and dissolved Pb, Fe and Mn concentrations for the surface sediment (0-2 cm) slurries from stations 3B and MIS. The expected, nearly immediate increase in dissolved metal concentrations due to porewater dilution was calculated from measured concentrations in porewater [17,28] and from sediment porosity. The experimental data support important porewater contribution to the measured dissolved Fe and Mn concentrations in the batch experiment, as suboxic porewater was enriched in Fe^{II} and Mn^{II}, due to reactive Fe and Mn (oxy)hydroxides reduction by early diagenesis [17]. If Fe is rapidly scavenged (~15 min) due to known fast kinetics of reoxydation and precipitation in oxygenated seawater, Mn remained in dissolved phase for a longer time (~7 h) before being removed following the same processes. Such differences in Fe and Mn precipitation kinetics have already been observed in previous studies [58,59]. Concerning Pb remobilisation kinetics, the rapid release within 5 min, noticeable in most of the performed experiments (Fig. 5B and A.3), was not due to porewater contribution but could be attributed to a fast solid/liquid repartitioning, describable by a K_d partition coefficient [60]. This weakly-bound Pb fraction was assumed as the "labile" fraction whose release mechanism was related to cation exchange reactions [61]. Then, Pb appeared to be continuously released, probably from a more strongly particle-bound fraction [61] until ~7 h, after which Mn oxides started to precipitate. As Mn oxides are known to be efficient Pb carrying phases in sediments [62], Pb adsorption onto freshly precipitated Mn oxyhydroxides could explain the systematic Pb removal [63] observed for the longest contact times with all the studied surface sediments (Fig. 5B). The noticeable discrepancy observed for the deep/anoxic sediments from station MIS (Fig. 5B) could be attributed to the involvement of sulfidic phases, acting as binding phases prior to be reoxydized within minutes to hours [61,62]. This scenario suggests that Pb

precipitated and definitively fixed as diagenetic sulphides in anoxic sediments, could be partially released into the oxic water column within hours or days of resuspension.

The Pb isotopic composition of seawater during MIS sediment resuspension experiments corresponded to that of sedimentary Pb (Fig. 5B). This observation supports mobility of the sedimentary ^{anthropogenic}Pb stock being desorbed from particles and the consecutive impact on the ecosystem quality.

Therefore, any scenario inducing resuspension of Pb contaminated surface sediments will lead to a non-negligible Pb remobilisation, resulting in both increased particulate and dissolved Pb concentrations in the water column, which can further be transferred to and bio-accumulated by filter feeder organisms such as mussels. In coastal systems such as the Toulon Bay, which are constantly submitted to various forcing and sediment perturbation (e.g. storm/waves, tidal current, bioturbation, ship traffic/trawling, dredging, harbour infrastructure building, …), such processes are more than probable to play an important role on surface water quality, although it remains difficult to quantify their respective contributions. It is, however, evident from sediment contamination mapping and hydrodynamic studies that resuspension processes actually participate to the export of contaminants to the open sea [20,23], probably inducing noticeable toxicological/ecological impacts on various marine organisms [64–66].

The obtained results on Pb distribution in sediments, water and stable Pb isotopic signatures clearly evidenced the impact of historical pollution and the dispersion of this pollutant stock over the whole bay, together with other accompanying pollutants (e.g. Hg). A specific ^{anthropogenic}Pb isotopic signature in the Toulon Bay was revealed (^{206}Pb/^{207}Pb ~ 1.166±0.003 and ^{206}Pb/^{208}Pb ~ 0.475±0.001), probably resulting from the multiplicity of Pb sources used by Navy in the last century. Different factors, either natural (storms, waves, bioturbation) or anthropogenic (ship movement, dredging) most probably explain Pb export (i) to the more distal surface sediments of the bay and also (ii) to other compartments such as water column through remobilisation (as illustrated by sediment resuspension experiments) and biota. The combination of the spatial distribution of Pb concentrations in surface water and sediments of the Toulon Bay, isotope signatures in water, sediment and mussels and our observations on Pb release during sediment resuspension clearly supports Pb transfer between these compartments. This study confirmed the vulnerability of the Toulon Bay ecosystems in particular, and those of many coastal areas worldwide, where Pb contamination may affect

both ecosystem and Human health, given that Toulon Bay mussels are still consumed, although their Pb levels equal or exceed European safety thresholds.

ACKNOWLEDGEMENTS:

This study was performed in the framework of MerMex-WP3-C3A research program (part of the international IMBER project), CARTOCHIM and CARTOC research programs (funded by "Toulon-Provence-Méditerranée (TPM)", the "Région PACA", and "l'Agence de l'Eau Rhône-Méditerranée et Corse"), PREVENT research program (funded by "Toulon University", "Toulon-Provence-Méditerranée", and the "Conseil Départemental du Var"). The authors acknowledge support from FEDER (Fonds Européen de Développement Régional) and the "Région Aquitaine". The authors wish to thank the French Navy for diving and sampling assistance, Dr. Omanović for HR ICP-MS analysis (RBI, Zagreb, Croatia), Dr. C. Dufresne and Dr. C. Duffa (IRSN, La Seyne s/Mer, France) for tributary particle sampling and conditioning, Dr. B. Oursel (IMBE, Marseille, France) for sampling assistance. The authors wish to thank the 3 anonymous reviewers for their helpful comments.

SUPPORTING INFORMATION

Table S1: The Pb stable isotope ratios ($^{206}Pb/^{207}Pb$ and $^{206}Pb/^{208}Pb$) of different Pb sources

Figure S1: Photos of coal block and bulk Pb plate from the "Magenta" French Navy battleship

Figure S2: Pb stable isotope ratios and Pb content depth profiles at stations 3B and 23

Figure S3: $^{206}Pb/^{208}Pb$ ratio as a function of $^{206}Pb/^{207}Pb$ for various Pb sources

Figure S4: Time variation of pH, dissolved Pb, Fe and Mn concentrations released during sediment resuspension

Figure S5: Contribution of $^{anthropogenic}Pb$ source of Toulon Bay's surface sediments

Figure S6: Relationship observed between the total and dissolved Pb at 40 stations around Toulon bay

This information is available free of charge via the Internet at http://pubs.acs.org/

499 REFERENCES

500 (1) Callender, E. Heavy Metals in the Environment — Historical Trends. In *Treatise on*
501 *Geochemistry*; Turekian, K. K., Holland, H. D., Eds.; Elsevier Ltd, 2003; Vol. 5, pp
502 67–105.

503 (2) Elbaz-Poulichet, F.; Dezileau, L.; Freydier, R.; Cossa, D.; Sabatier, P. A 3500-year
504 record of Hg and Pb contamination in a mediterranean sedimentary archive (the Pierre
505 Blanche Lagoon, France). *Environ. Sci. Technol.* **2011**, *45*, 8642–8647.

506 (3) Reimann, C.; Caritat, P. *Chemical Elements in the Environment*; Springer, Berlin,
507 1998.

508 (4) Hopper, J. F.; Ross, H. B.; Sturge, W. T.; Barrie, L. A. Regional source discrimination
509 of atmospheric aerosols in Europe using the isotopic composition of lead. *Tellus* **1991**,
510 *43B*, 45–60.

511 (5) Monna, F.; Othman, D. Ben; Luck, J. Pb isotopes and Pb, Zn and Cd concentrations in
512 the rivers feeding a coastal pond (Thau, southern France): constraints on the origin (s)
513 and flux (es) of metals. *Sci. Total Environ.* **1995**, *166*, 19–34.

514 (6) Cossa, D.; Buscail, R.; Puig, P.; Chiffoleau, J.-F.; Radakovitch, O.; Jeanty, G.;
515 Heussner, S. Origin and accumulation of trace elements in sediments of the
516 northwestern Mediterranean margin. *Chem. Geol.* **2014**, *380*, 61–73.

517 (7) Besada, V.; Manuel Andrade, J.; Schultze, F.; José González, J. Monitoring of heavy
518 metals in wild mussels (Mytilus galloprovincialis) from the Spanish North-Atlantic
519 coast. *Cont. Shelf Res.* **2011**, *31*, 457–465.

520 (8) Couture, R.-M.; Chiffoleau, J.-F.; Auger, D.; Claisse, D.; Gobeil, C.; Cossa, D.
521 Seasonal and decadal variations in lead sources to eastern North Atlantic mussels.
522 *Environ. Sci. Technol.* **2010**, *44*, 1211–1216.

(9) Bollhöfer, A. Stable lead isotope ratios and metals in freshwater mussels from a uranium mining environment in Australia's wet-dry tropics. *Appl. Geochemistry* **2012**, *27*, 171–185.

(10) Claisse, D. Chemical contamination of French coasts: the results of a ten years mussel watch. *Mar. Pollut. Bull.* **1989**, *20*, 217–218.

(11) Kimbrough, K. L.; Johnson, W. E.; Lauenstein, G. G.; Chrstensen, J. D.; Apeti, D. A. *An assessment of two decades of contaminant monitoring in the nation's coastal zone. Silver Spring, MD. NOAA Technical Memorandum NOS NCCOS 74*; Silver Spring, MD, 2008.

(12) Turner, A. Marine pollution from antifouling paint particles. *Mar. Pollut. Bull.* **2010**, *60*, 159–171.

(13) Turner, A. Mobilisation and bioaccessibility of lead in paint from abandoned boats. *Mar. Pollut. Bull.* **2014**, *89*, 35–39.

(14) Karuppiah, M.; Gupta, G. Chronological changes in toxicity of and heavy metals in sediments of two Chesapeake Bay tributaries. *J. Hazard. Mater.* **1998**, *59*, 159–166.

(15) Louriño-Cabana, B.; Lesven, L.; Charriau, A.; Billon, G.; Ouddane, B.; Boughriet, A. Potential risks of metal toxicity in contaminated sediments of Deûle river in northern France. *J. Hazard. Mater.* **2011**, *186*, 2129–2137.

(16) Rigaud, S.; Radakovitch, O.; Couture, R.-M.; Deflandre, B.; Cossa, D.; Garnier, C.; Garnier, J.-M. Mobility and fluxes of trace elements and nutrients at the sediment–water interface of a lagoon under contrasting water column oxygenation conditions. *Appl. Geochemistry* **2013**, *31*, 35–51.

(17) Dang, D. H.; Tessier, E.; Lenoble, V.; Durrieu, G.; Omanović, D.; Mullot, J.-U.; Pfeifer, H.-R.; Mounier, S.; Garnier, C. Key parameters controlling arsenic dynamics in coastal sediments: an analytical and modeling approach. *Mar. Chem.* **2014**, *161*, 34–46.

548 (18) Lesven, L.; Lourino-Cabana, B.; Billon, G.; Recourt, P.; Ouddane, B.; Mikkelsen, O.;
549 Boughriet, a. On metal diagenesis in contaminated sediments of the Deûle river
550 (northern France). *Appl. Geochemistry* **2010**, *25*, 1361–1373.

551 (19) Dang, D. H.; Lenoble, V.; Durrieu, G.; Mullot, J.-U.; Mounier, S.; Garnier, C.
552 Sedimentary dynamics of coastal organic matter: An assessment of the porewater
553 size/reactivity model by spectroscopic techniques. *Estuar. Coast. Shelf Sci.* **2014**, *151*,
554 100–111.

555 (20) Pougnet, F.; Schäfer, J.; Dutruch, L.; Garnier, C.; Tessier, E.; Dang, D. H.; Lanceleur,
556 L.; Mullot, J.-U.; Lenoble, V.; Blanc, G. Sources and historical record of tin and butyl-
557 tin species in a Mediterranean bay (Toulon Bay, France). *Environ. Sci. Pollut. Res. Int.*
558 **2014**, *21*, 6640–6651.

559 (21) Tessier, E.; Garnier, C.; Mullot, J.-U.; Lenoble, V.; Arnaud, M.; Raynaud, M.;
560 Mounier, S. Study of the spatial and historical distribution of sediment inorganic
561 contamination in the Toulon bay (France). *Mar. Pollut. Bull.* **2011**, *62*, 2075–2086.

562 (22) Cossa, D.; Garnier, C.; Buscail, R.; Elbaz-Poulichet, F.; Mikac, N.; Patel-Sorrentino,
563 N.; Tessier, E.; Rigaud, S.; Lenoble, V.; Gobeil, C. A Michaelis–Menten type equation
564 for describing methylmercury dependence on inorganic mercury in aquatic sediments.
565 *Biogeochemistry* **2014**, *119*, 35–43.

566 (23) Dufresne, C.; Duffa, C.; Rey, V. Wind-forced circulation model and water exchanges
567 through the channel in the Bay of Toulon. *Ocean Dyn.* **2014**, *64*, 209–224.

568 (24) Andral, B.; Stanisiere, J. Y.; Sauzade, D.; Damier, E.; Thebault, H.; Galgani, F.;
569 Boissery, P. Monitoring chemical contamination levels in the Mediterranean based on
570 the use of mussel caging. *Mar. Pollut. Bull.* **2004**, *49*, 704–712.

571 (25) Casas, S.; Gonzalez, J.-L.; Andral, B.; Cossa, D. Relation between metal concentration
572 in water and metal content of marine mussels (Mytilus galloprovincialis): impact of
573 physiology. *Environ. Toxicol. Chem.* **2008**, *27*, 1543–1552.

(26) Phillips, J.; Russell, M.; Walling, D. Time-integrated sampling of fluvial suspended sediment: a simple methodology for small catchments. *Hydrol. Process.* **2000**, *14*, 2589–2602.

(27) Oursel, B.; Garnier, C.; Pairaud, I.; Omanović, D.; Durrieu, G.; Syakti, a. D.; Le Poupon, C.; Thouvenin, B.; Lucas, Y. Behaviour and fate of urban particles in coastal waters: Settling rate, size distribution and metals contamination characterization. *Estuar. Coast. Shelf Sci.* **2014**, *138*, 14–26.

(28) Dufresne, C. Compréhension et analyse des processus hydrosédimentaires dans la baie de Toulon. Apport à la modélisation de la dispersion des radionucléides, Université de Toulon, 2014.

(29) Dang, D. H.; Lenoble, V.; Durrieu, G.; Omanović, D.; Mullot, J.-U.; Mounier, S.; Garnier, C. Seasonal variations of coastal sedimentary trace metals cycling: Insight on the effect of manganese and iron (oxy)hydroxides, sulphide and organic matter. *Mar. Pollut. Bull.* **2015**, *92*, 113–124.

(30) Louis, Y.; Garnier, C.; Lenoble, V.; Mounier, S.; Cukrov, N.; Omanović, D.; Pižeta, I. Kinetic and equilibrium studies of copper-dissolved organic matter complexation in water column of the stratified Krka River estuary (Croatia). *Mar. Chem.* **2009**, *114*, 110–119.

(31) Larrose, A.; Coynel, A.; Schäfer, J.; Blanc, G.; Massé, L.; Maneux, E. Assessing the current state of the Gironde Estuary by mapping priority contaminant distribution and risk potential in surface sediment. *Appl. Geochemistry* **2010**, *25*, 1912–1923.

(32) Lenoble, V.; Omanović, D.; Garnier, C.; Mounier, S.; Đonlagić, N.; Le Poupon, C.; Pižeta, I. Distribution and chemical speciation of arsenic and heavy metals in highly contaminated waters used for health care purposes (Srebrenica, Bosnia and Herzegovina). *Sci. Total Environ.* **2013**, *443*, 420–428.

(33) Petit, J. C. J.; Schäfer, J.; Coynel, A.; Blanc, G.; Deycard, V. N.; Derriennic, H.; Lanceleur, L.; Dutruch, L.; Bossy, C.; Mattielli, N. Anthropogenic sources and

biogeochemical reactivity of particulate and dissolved Cu isotopes in the turbidity gradient of the Garonne River (France). *Chem. Geol.* **2013**, *359*, 125–135.

(34) Oursel, B.; Garnier, C.; Durrieu, G.; Mounier, S.; Omanović, D.; Lucas, Y. Dynamics and fates of trace metals chronically input in a Mediterranean coastal zone impacted by a large urban area. *Mar. Pollut. Bull.* **2013**, *69*, 137–149.

(35) Danielsson, L.; Magnusson, B. Trace metal determinations in estuarine waters by electrothermal atomic absorption spectrometry after extraction of dithiocarbamate complexes into freon. *Anal. Chim. Acta* **1982**, *144*, 183–188.

(36) Chiffoleau, J.; Auger, D.; Boutier, B.; Rozuel, E.; Truquet, I. *Dosage de certains métaux dans les sédiments et la matière en suspension par absorption atomique.*; Edition Ifremer, 2004.

(37) Duffa, C.; Dufois, F.; Coudray, S. An operational model to simulate post-accidental radionuclide transfers in Toulon marine area: preliminary development. *Ocean Dyn.* **2011**, *61*, 1811–1821.

(38) Spada, L.; Annicchiarico, C. Heavy metals monitoring in mussels Mytilus galloprovincialis from the Apulian coasts (Southern Italy). *Mediterr. Mar. Sci.* **2013**, *14*, 99–108.

(39) Labonne, M.; Othman, D. Ben; Luck, J. Pb isotopes in mussels as tracers of metal sources and water movements in a lagoon (Thau Basin, S. France). *Chem. Geol.* **2001**, *181*, 181–191.

(40) Benedicto, J.; Andral, B.; Martínez-Gómez, C.; Guitart, C.; Deudero, S.; Cento, A.; Scarpato, A.; Caixach, J.; Benbrahim, S.; Chouba, L.; et al. A large scale survey of trace metal levels in coastal waters of the Western Mediterranean basin using caged mussels (Mytilus galloprovincialis). *J. Environ. Monit.* **2011**, *13*, 1495–1505.

(41) INERIS. *Synthèse des valeurs réglementaires pour les substances chimiques, en vigueur dans l'eau, les denrées alimentaires et dans l'air en France au 1er décembre*

627 *2011.*; Rapport réalisé pour le Ministère de l'Écologie, du Développement Durable, des
628 Transports et du Logement, Direction Générale de la prévention des risques (DGPR),
629 2013.

630 (42) Ifremer. *Réseau de suivi lagunaire du Languedoc-Roussillon: Bilan des résultats*
631 *2005.*; Raport RSL-06/2006, 2006.

632 (43) Monna, F.; Lancelot, J.; Croudace, I. W.; Cundy, A. B.; Lewis, J. T. Pb Isotopic
633 Composition of Airborne Particulate Material from France and the Southern United
634 Kingdom: Implications for Pb Pollution Sources in Urban Areas. *Environ. Sci.*
635 *Technol.* **1997**, *31*, 2277–2286.

636 (44) Markich, S.; Jeffree, R. Absorption of divalent trace metals as analogues of calcium by
637 Australian freshwater bivalves: an explanation of how water hardness reduces metal
638 toxicity. *Aquat. Toxicol.* **1994**, *29*, 257–290.

639 (45) Roditi, H. A.; Fisher, N. S.; Sañudo-Wilhelmy, S. A. Uptake of dissolved organic
640 carbon and trace elements by zebra mussels. *Nature* **2000**, *407*, 78–80.

641 (46) Wang, W.-X.; Fisher, N. S.; Luoma, S. N. Assimilation of trace elements ingested by
642 the mussel Mytilus edulis:effects of algal food abundance. *Mar. Ecol. Prog. Ser.* **1995**,
643 *129*, 165–176.

644 (47) Gagnon, C.; Fisher, N. S. The bioavailability of sediment-bound Cd, Co, and Ag to the
645 mussel Mytilus edulis. *Can. J. Fish. Aquat. Sci.* **1997**, *54*, 147–156.

646 (48) Ke, C.; Wang, W.-X. Trace metal ingestion and assimilation by the green mussel Perna
647 viridis in a phytoplankton and sediment mixture. *Mar. Biol.* **2002**, *140*, 327–335.

648 (49) Chong, K.; Wang, W. Bioavailability of sediment-bound Cd, Cr and Zn to the green
649 mussel Perna viridis and the Manila clam Ruditapes philippinarum. *J. Exp. Mar. Bio.*
650 *Ecol.* **2000**, *255*, 75–92.

(50) Strady, E.; Schafer, J.; Baudrimont, M.; Blanc, G. Tracing cadmium contamination kinetics and pathways in oysters (Crassostrea gigas) by multiple stable Cd isotope spike experiments. *Ecotoxicol. Environ. Saf.* **2011**, *74*, 600–606.

(51) Morley, N. H.; Burton, J. D.; Tankere, S. P. C.; Martin, J.-M. Distribution and behaviour of some dissolved trace metals in the western Mediterranean Sea. *Deep Sea Res. Part II Top. Stud. Oceanogr.* **1997**, *44*, 675–691.

(52) Jean, N.; Dumont, E.; Durrieu, G.; Balliau, T.; Jamet, J.-L.; Personnic, S.; Garnier, C. Protein expression from zooplankton communities in a metal contaminated NW mediterranean coastal ecosystem. *Mar. Environ. Res.* **2012**, *80*, 12–26.

(53) Botelho, C. M. S.; Boaventura, R. a. R.; Gonçalves, M. L. S. S. Interactions of Pb(II) with particles of a polluted river. *Anal. Chim. Acta* **2002**, *462*, 73–85.

(54) Baskaran, M.; Santschi, P. H. The role of particles and colloids in the transport of radionuclides in coastal environments of Texas. *Mar. Chem.* **1993**, *43*, 95–114.

(55) Gallon, C.; Tessier, A.; Gobeil, C.; Alfaro-De La Torre, M. Modeling diagenesis of lead in sediments of a Canadian Shield lake. *Geochim. Cosmochim. Acta* **2004**, *68*, 3531–3545.

(56) Caetano, M.; Madureira, M.-J.; Vale, C. Metal remobilisation during resuspension of anoxic contaminated sediment: Short-term laboratory study. *Water, Air, Soil Pollut.* **2002**, *143*, 23–40.

(57) Superville, P.-J.; Prygiel, E.; Magnier, A.; Lesven, L.; Gao, Y.; Baeyens, W.; Ouddane, B.; Dumoulin, D.; Billon, G. Daily variations of Zn and Pb concentrations in the Deûle River in relation to the resuspension of heavily polluted sediments. *Sci. Total Environ.* **2014**, *470*, 600–607.

(58) Morgan, J. J. Kinetics of reaction between O2 and Mn(II) species in aqueous solutions. *Geochim. Cosmochim. Acta* **2005**, *69*, 35–48.

(59) Rose, A. L.; Waite, T. D. Kinetics of hydrolysis and precipitation of ferric iron in seawater. *Environ. Sci. Technol.* **2003**, *37*, 3897–3903.

(60) Turner, A.; Crussell, M.; Millward, G. E.; Cobelo-Garcia, A.; Fisher, A. S. Adsorption Kinetics of Platinum Group Elements in River Water. *Environ. Sci. Technol.* **2006**, *40*, 1524–1531.

(61) Cappuyns, V.; Swennen, R. The application of pH(stat) leaching tests to assess the pH-dependent release of trace metals from soils, sediments and waste materials. *J. Hazard. Mater.* **2008**, *158*, 185–195.

(62) Eggleton, J.; Thomas, K. V. A review of factors affecting the release and bioavailability of contaminants during sediment disturbance events. *Environ. Int.* **2004**, *30*, 973–980.

(63) Elbaz-Poulichet, F.; Holliger, P.; Wen Huang, W.; Martin, J.-M. Lead cycling in estuaries, illustrated by the Gironde estuary, France. *Nature* **1984**, *308*, 409–414.

(64) Roberts, D. A. Causes and ecological effects of resuspended contaminated sediments (RCS) in marine environments. *Environ. Int.* **2012**, *40*, 230–243.

(65) Vale, C.; Ferreira, a; Micaelo, C.; Caetano, M.; Pereira, E.; Madureira, M.; Ramalhosa, E. Mobility of contaminants inrelation to dredging operations in a mesotidal estuary (Tagus Estuary, Portugal). *Water Sci. Technol.* **1998**, *37*, 25–31.

(66) Vicente-Martorell, J. J.; Galindo-Riaño, M. D.; García-Vargas, M.; Granado-Castro, M. D. Bioavailability of heavy metals monitoring water, sediments and fish species from a polluted estuary. *J. Hazard. Mater.* **2009**, *162*, 823–836.

TABLE

Table 1: Summary of Pb contents, $^{206}Pb/^{207}Pb$ and $^{206}Pb/^{208}Pb$ ratios in semi-total extracts expressed in average (number of sample) and the variation range (min-max) in surface and cored sediments. The specific Pb isotope compositions of lead issued from anthropogenic, natural and gasoline sources are presented as $^{anthropogenic}Pb$, $^{natural}Pb$ and $^{gasoline}Pb$. The $^{natural}Pb$ and $^{gasoline}Pb$ signatures are gathered from literature, see Table S1 for detailed values and citations.

		Pb content (µg g^{-1})	$^{206}Pb/^{207}Pb$	$^{206}Pb/^{208}Pb$
Surface sediments	Average	107 (n = *54*)	1.168 (n = *34*)	0.475 (n = *34*)
	Range (min-max)	15-467	1.156-1.180	0.474-0.478
St. MIS	Average	907 (n = *28*)	1.164 (n = *7*)	0.475 (n = *7*)
	Range (min-max)	377-1310	1.156-1.172	0.474-0.476
St. 3B	Average	201 (n = *23*)	1.166 (n = *7*)	0.475 (n = *7*)
	Range (min-max)	146-265	1.162-1.1700	0.474-0.476
St. 12	Average	179 (n = *29*)	1.174 (n = *29*)	0.476 (n = *29*)
	Range (min-max)	70-423	1.165-1.180	0.475-0.479
St. 15	Average	50 (n = *28*)	1.179 (n = 14)	0.478 (n = 14)
	Range (min-max)	14-118	1.164-1.197	0.475-0.482
St. 23	Average	41.9 (n = *20*)	1.175 (n = *7*)	0.476 (n = *7*)
	Range (min-max)	15-78	1.165-1.189	0.473-0.478
$^{anthropogenic}Pb$	n = 14		1.165±0.004	0.475±0.001
$^{natural}Pb$	n = 16		1.195±0.014	0.483±0.003
$^{gasoline}Pb$[43]	n = 9		1.084±0.010	0.458±0.002

FIGURES

Figure 1: Map of the studied site with the main anthropogenic activities and location of the 54 sampled surface (0-5 cm) sediments (open square), 5 50-cm interface sediment cores (circle) and 6 seawater samples collected for Pb isotopes analysis (open diamond). The contour plot represents the total Pb content in surface sediments.

Figure 2: Pb stable isotope ratios ($^{206}Pb/^{207}Pb$ and $^{206}Pb/^{208}Pb$, circle and square, respectively) and Pb content depth profiles (diamond) from 50-cm interface core collected at stations MIS, 12 and 15. The full and open symbols respectively represent total and HCl-extracted fractions. The filled areas with increasing grey scale indicate specific signature of industrial Pb, leaded gasoline and natural Pb, respectively. The full and dashed lines represent the variation range and the average value of the Pb isotopes ratios recorded in surface sediments (n = 54) of Toulon Bay, respectively.

Figure 3: Pb content in farmed mussels sampled in summer/fall and winter/spring periods (close and open triangle, respectively). The grey diamond, circle and square symbols represent wild mussels sampled in 2014 at stations MIS, 12 and Milhaud dock, respectively. The filled areas represent guideline levels in mussels from American coast [11]. The dotted line represents the range of Pb content in Mediterranean mussels [24,39]. $^{206}Pb/^{207}Pb$ ratio (grey symbols) in mussels is compared to the average and range of $^{206}Pb/^{207}Pb$ ratio variation in surface sediments (full and dashed lines). The calculated contribution of $^{anthropogenic}Pb$ signature in mussel is shown (red line).

Figure 4: $^{206Pb}/^{208}Pb$ ratio as a function $^{206}Pb/^{207}Pb$ ratio for (A) Toulon Bay sediments (circles and squares illustrating interface sediment cores and surface sediments, respectively), tributaries particles (cross, symbol size as a function of Pb total content), "Anzin" coal block (star) and "Magenta" French Navy battleship's Pb plate (hexagone), (B) seawater (blue triangles), mussels (reverse triangles, grey square, circle and diamond) samples in comparison to the range of variation of various Pb sources from literature (Table S1 and Figure S2).

741

742 **Figure 5**: (A) Dissolved Pb concentration in surface seawater at 40 stations of Toulon Bay
743 (February 2014). A contour map was generated by kriging method and the scale layers
744 represent the statistical distribution (centiles) of the concentration range. (B) Dissolved Pb
745 concentration (and $^{206}Pb/^{207}Pb$ ratio) remobilized during sediments resuspension simulation
746 experiments using sediments from stations MIS, 3B, 12 and 15 as a function of time. Open
747 and close symbols represent surface and deep sediments, respectively (see text for more
748 details).

749

750

Table 1:

		Pb content (μg g^{-1})	$^{206}Pb/^{207}Pb$	$^{206}Pb/^{208}Pb$
Surface sediments	Average (sample number)	107 (34)	1.168 (34)	0.475 (34)
	Range (min-max)	15-467	1.156-1.180	0.474-0.478
St. MIS	Average	907 (28)	1.164 (7)	0.475 (7)
	Range (min-max)	377-1310	1.156-1.172	0.474-0.476
St. 3B	Average	201 (23)	1.166 (7)	0.475 (7)
	Range (min-max)	146-265	1.162-1.1700	0.474-0.476
St. 12	Average	179 (29)	1.174 (29)	0.476 (29)
	Range (min-max)	70-423	1.165-1.180	0.475-0.479
St. 15	Average	50 (28)	1.179 (14)	0.478 (14)
	Range (min-max)	14-118	1.164-1.197	0.475-0.482
St. 23	Average	41.9 (20)	1.175 (7)	0.476 (7)
	Range (min-max)	15-78	1.165-1.189	0.473-0.478
$^{anthropogenic}Pb$	n = 14		1.165±0.004	0.475±0.001
$^{natural}Pb$	n = 16		1.195±0.014	0.483±0.003
$^{gasoline}Pb$[43]	n = 9		1.084±0.010	0.458±0.002

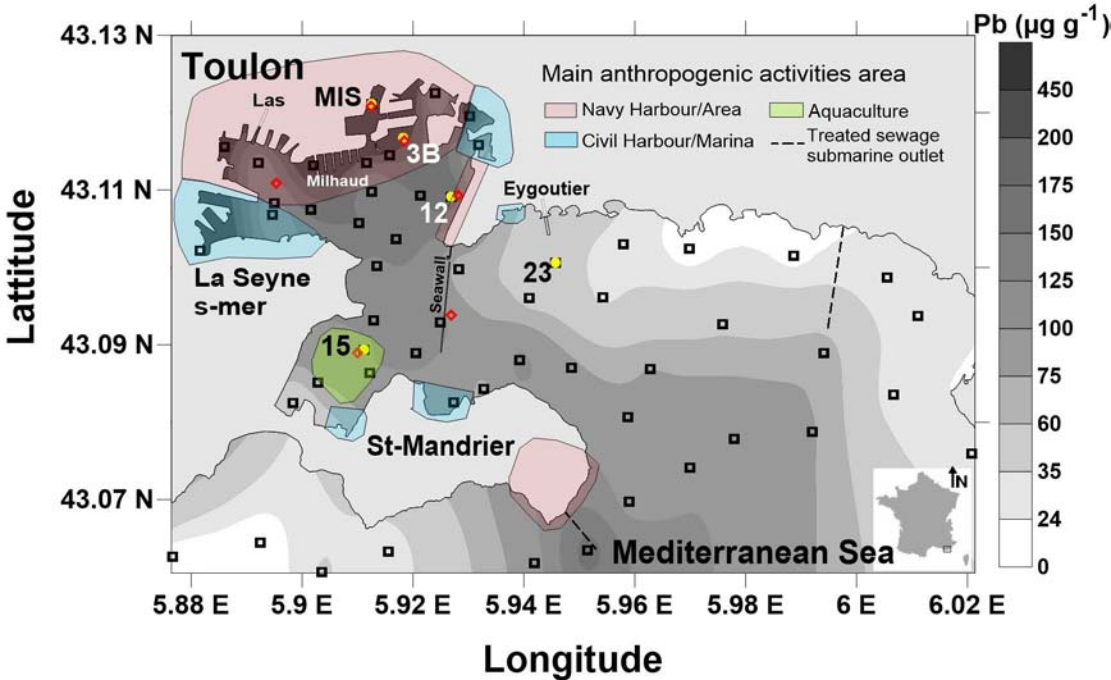
Toulon
Las
MIS
3B
Milhaud
12
Eygoutier
La Seyne
s-mer
Seawall
23
15
St-Mandrier
Mediterranean Sea
N
Main anthropogenic activities area
Navy Harbour/Area
Aquaculture
Civil Harbour/Marina
Treated sewage
submarine outlet
Pb (µg g-1)
450
200
175
150
125
100
75
60
35
24
0
43.13 N
43.11 N
43.09 N
43.07 N
Lattitude
5.88 E
5.9 E
5.92 E
5.94 E
5.96 E
5.98 E
6 E
6.02 E
Longitude

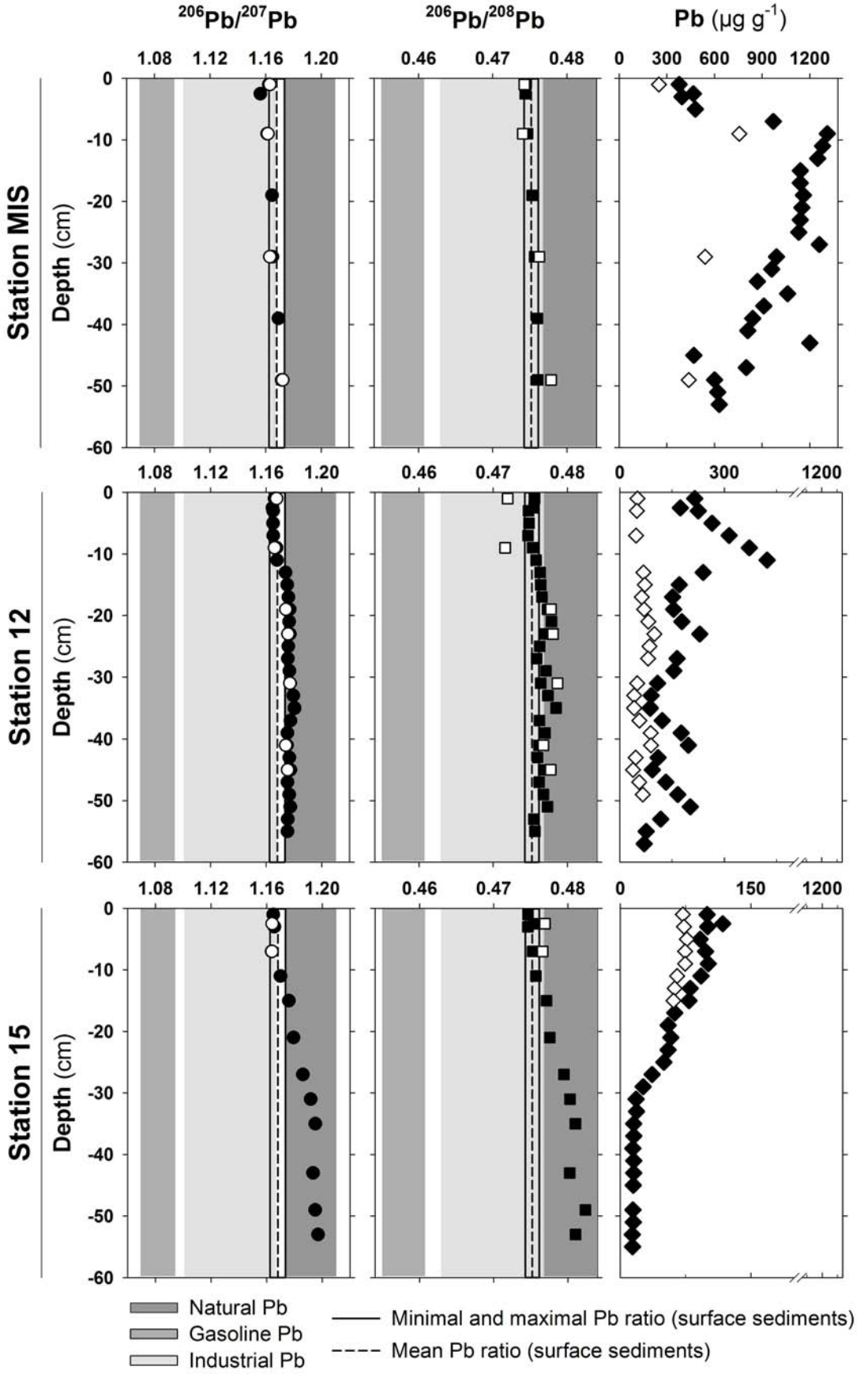
$^{206}Pb/^{207}Pb$
$^{206}Pb/^{208}Pb$
Pb (µg g^{-1})
Station MIS
Station 12
Station 15
Depth (cm)
1.08 1.12 1.16 1.20
0.46 0.47 0.48
0 300 600 900 1200
0 -10 -20 -30 -40 -50 -60
0 300 1200
0 150 1200
Natural Pb
Gasoline Pb
Industrial Pb
Minimal and maximal Pb ratio (surface sediments)
Mean Pb ratio (surface sediments)

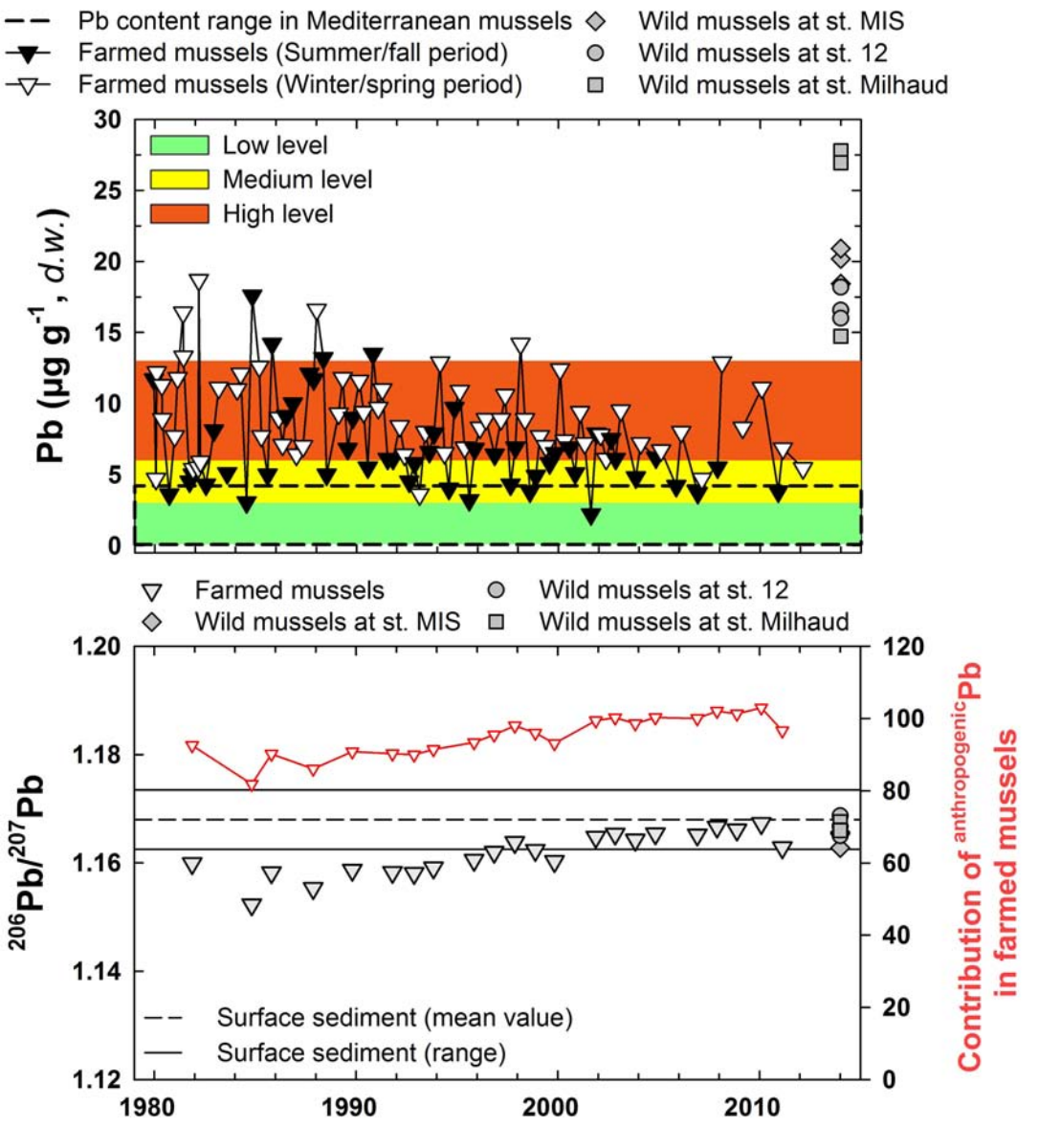
Pb content range in Mediterranean mussels
Farmed mussels (Summer/fall period)
Farmed mussels (Winter/spring period)
Wild mussels at st. MIS
Wild mussels at st. 12
Wild mussels at st. Milhaud
Low level
Medium level
High level
Pb (µg g-1, d.w.)
30
25
20
15
10
5
0
Farmed mussels
Wild mussels at st. MIS
Wild mussels at st. 12
Wild mussels at st. Milhaud
206Pb/207Pb
1.20
1.18
1.16
1.14
1.12
Surface sediment (mean value)
Surface sediment (range)
120
100
80
60
40
20
0
Contribution of anthropogenic Pb in farmed mussels
1980
1990
2000
2010

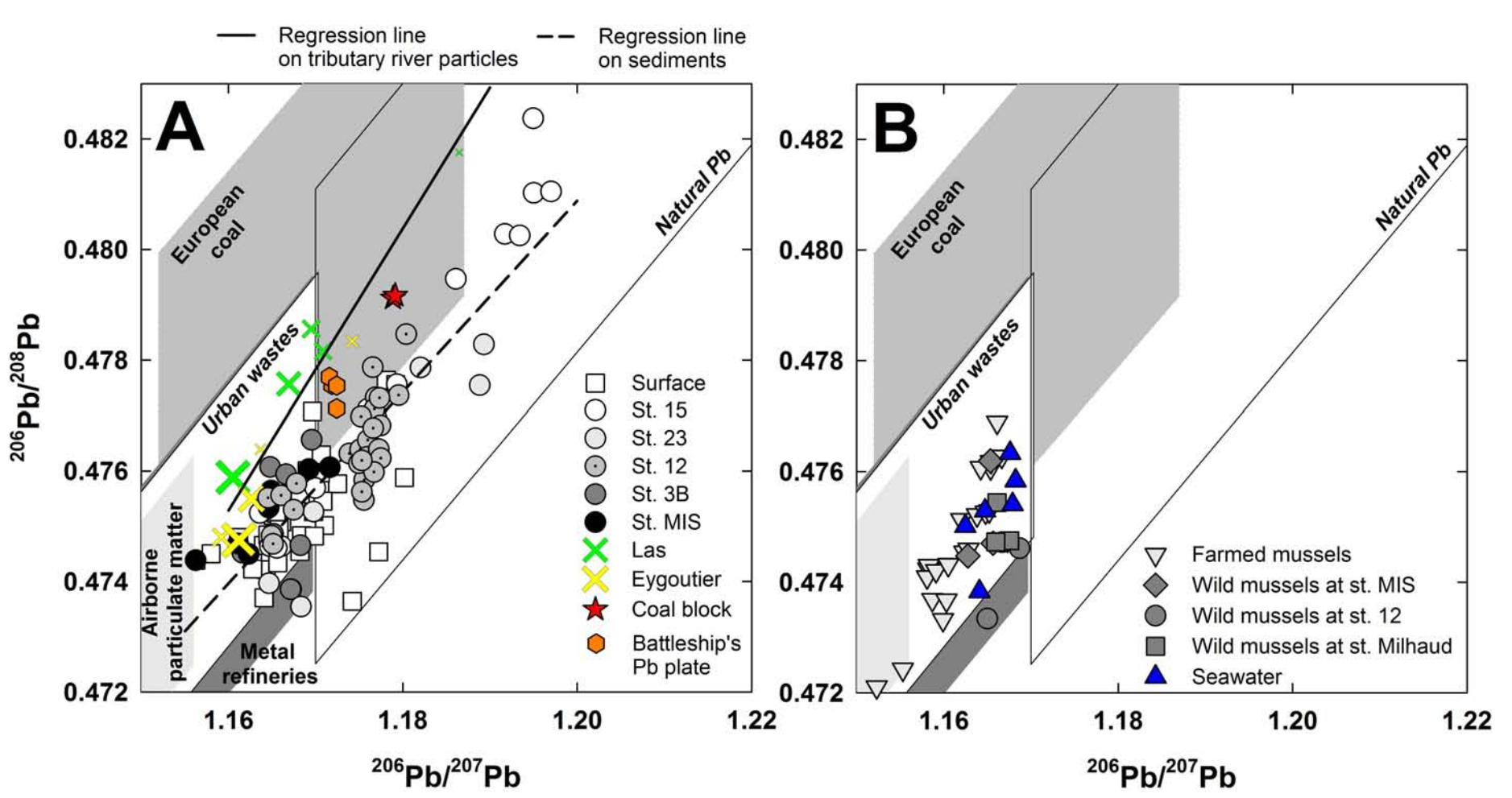
Regression line on tributary river particles
Regression line on sediments
A
B
European coal
Urban wastes
Natural Pb
Airborne particulate matter
Metal refineries
Surface
St. 15
St. 23
St. 12
St. 3B
St. MIS
Las
Eygoutier
Coal block
Battleship's Pb plate
Farmed mussels
Wild mussels at st. MIS
Wild mussels at st. 12
Wild mussels at st. Milhaud
Seawater
0.482
0.480
0.478
0.476
0.474
0.472
1.16
1.18
1.20
1.22
206Pb/208Pb
206Pb/207Pb

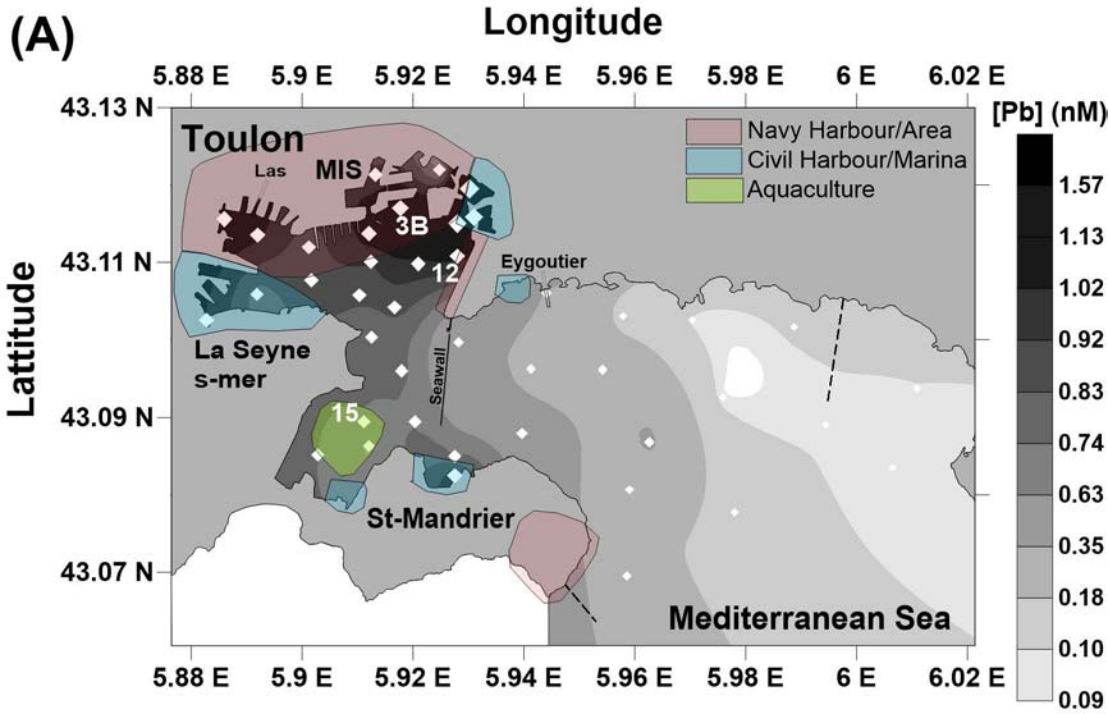
(A)
Longitude
5.88 E
5.9 E
5.92 E
5.94 E
5.96 E
5.98 E
6 E
6.02 E
Lattitude
43.13 N
43.11 N
43.09 N
43.07 N
Toulon
Las
MIS
3B
12
Eygoutier
La Seyne
s-mer
Seawall
15
St-Mandrier
Mediterranean Sea
Navy Harbour/Area
Civil Harbour/Marina
Aquaculture
[Pb] (nM)
1.57
1.13
1.02
0.92
0.83
0.74
0.63
0.35
0.18
0.10
0.09

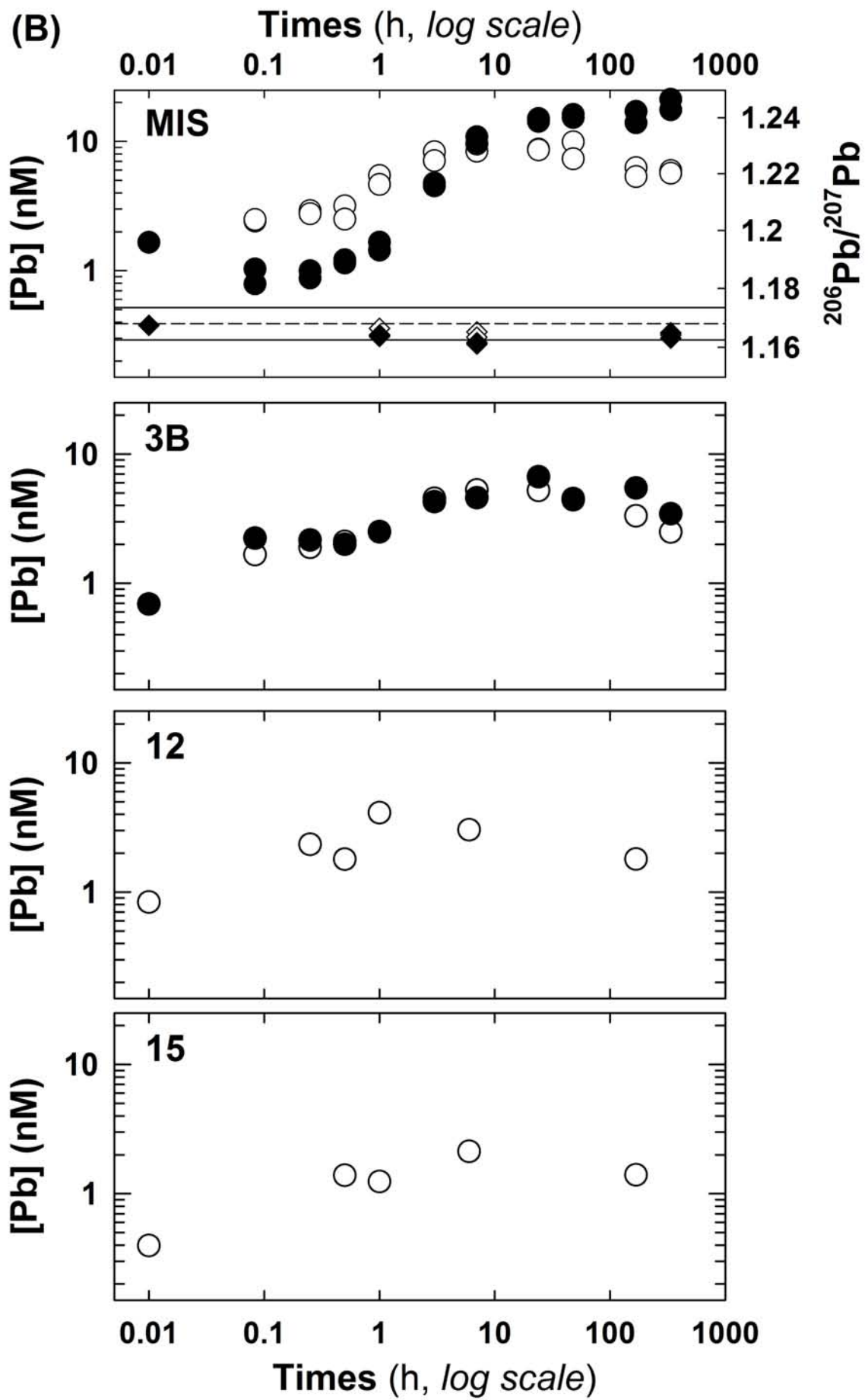
(B)
Times (h, log scale)
0.01
0.1
1
10
100
1000
MIS
3B
12
15
[Pb] (nM)
10
1
1.24
1.22
1.2
1.18
1.16
206Pb/207Pb
Times (h, log scale)

SUPPORTING INFORMATION

Manuscript Title: Evidencing the impact of coastal contaminated sediments on mussels through Pb stable isotopes composition

Authors Duc Huy Dang, Jörg Schäfer, Christophe Brach-Papa, Véronique Lenoble, Gaël Durrieu, Lionel Dutruch, Jean-Francois Chiffoleau, Jean-Louis Gonzalez, Gérard Blanc, Jean-Ulrich Mullot, Stéphane Mounier, Cédric Garnier*

*: corresponding author, email: cgarnier@univ-tln.fr

Number of pages: 11

Table S1: The Pb stable isotope ratios ($^{206}Pb/^{207}Pb$ and $^{206}Pb/^{208}Pb$) of different Pb sources

		$^{206}Pb/^{207}Pb$	$^{206}Pb/^{208}Pb$	Sample type	Reference
Natural		1.1730	0.4780	Sediment pre 1870	[1]
		1.1770	0.4810	Sediment pre 1870	[1]
		1.1970	0.4840	Pre/early industrial sediments	[2]
		1.2100	0.4864	Inland whole soil	[3]
		1.1900	0.4840	Emission pre1992	[3]
		1.2002	0.4833	Miocene rock and soil	[4]
		1.1783	0.4768	Pelagic sediments	[5]
		1.2028	0.4869	Miocene carbonate	[6]
		1.2046	0.4868	Palaeocene carbonate	[6]
		1.2019	0.4856	Soil carbonate	[6]
		1.2219	0.4872	Miocene silicate	[6]
		1.2043	0.4840	Palaeocene silicate	[6]
		1.2034	0.4848	Soil silicate.	[6]
	Mean	1.1947	0.4832		
	Minimal	1.1730	0.4768		
	Maximal	1.2219	0.4872		
Industrial emission		1.1158	0.4665	Airbone Particulate matter	[2]
		1.1219	0.4680	Airbone Particulate matter	[2]
		1.1094	0.4647	Airbone Particulate matter	[2]
		1.1091	0.4649	Airbone Particulate matter	[2]
		1.1123	0.4653	Airbone Particulate matter	[2]
		1.1124	0.4658	Airbone Particulate matter	[2]
		1.1212	0.4676	Airbone Particulate matter	[2]
		1.1219	0.4680	Airbone Particulate matter	[2]
		1.1211	0.4681	Airbone Particulate matter	[2]
		1.1159	0.4668	Airbone Particulate matter	[2]
		1.1181	0.4672	Airbone Particulate matter	[2]
		1.1069	0.4643	Airbone Particulate matter	[2]
		1.1008	0.4629	Airbone Particulate matter	[2]
		1.1221	0.4681	Airbone Particulate matter	[2]
		1.1342	0.4709	Airbone Particulate matter	[2]
		1.1319	0.4706	Airbone Particulate matter	[2]
		1.1042	0.4638	Airbone Particulate matter	[2]
		1.1453	0.4721	Airbone Particulate matter	[2]
		1.1150	0.4662	Emission post1992	[3]
		1.1530	0.4744	Emission Cairo	[3]
		1.1230	0.4671	Emission Turkey	[3]
	Mean	1.1196	0.4673		
	Minimal	1.1008	0.4629		
	Maximal	1.1530	0.4744		
Metal refineries		1.1549	0.4736	impacted soil-Pb, Zn refinery	[7]
		1.1576	0.4738	impacted soil-Pb, Zn refinery	[7]
		1.1569	0.4737	impacted soil-Pb, Zn refinery	[7]
		1.1563	0.4735	impacted soil-Pb, Zn refinery	[7]
		1.1565	0.4737	impacted soil-Pb, Zn refinery	[7]
		1.1579	0.4741	impacted soil-Pb, Zn refinery	[7]
		1.1565	0.4737	impacted soil-Pb, Zn refinery	[7]
		1.1574	0.4739	impacted soil-Pb, Zn refinery	[7]
		1.1583	0.4743	impacted soil-Pb, Zn refinery	[7]
		1.1575	0.4741	impacted soil-Pb, Zn refinery	[7]
		1.1584	0.4743	impacted soil-Pb, Zn refinery	[7]
		1.1667	0.4767	impacted soil-Pb, Zn refinery	[7]
		1.1633	0.4755	impacted soil-Pb, Zn refinery	[7]
		1.1040	0.4638	Slag-Pb, Zn refinery	[7]
		1.1305	0.4712	dust-Pb, Zn refinery	[7]

		1.1273	0.4706	dust-Pb, Zn refinery	[7]
		1.1176	0.4672	Fe-Mn metallurgy plant	[8]
		1.1064	0.4635	Fe-Mn metallurgy plant	[8]
		1.1099	0.4643	Fe-Mn metallurgy plant	[8]
		1.1336	0.4703	Lead smelter	[8]
		1.1323	0.4700	Lead smelter	[8]
	Mean	1.1438	0.4717		
	Minimal	1.1040	0.4635		
	Maximal	1.1667	0.4767		
Gasoline		1.0693	0.4550		[2]
		1.0806	0.4580		[2]
		1.0942	0.4604		[2]
		1.0942	0.4607		[2]
		1.0753	0.4565		[2]
		1.0878	0.4592		[2]
		1.0736	0.4563		[2]
		1.0856	0.4588		[2]
		1.0943	0.4602		[2]
	Mean	1.0839	0.4584		
	Minimal	1.0693	0.4550		
	Maximal	1.0943	0.4607		
European coal		1.1840	0.4799		[9]
		1.1809	0.4786		[10]
		1.1675	0.4778		[11]
		1.1700	0.4776		[12]
		1.1550	0.4779		[13]
		1.1800	0.4830		[14]
		1.1740	0.4820		[14]
		1.1810	0.4820		[14]
		1.1710	0.4800		[14]
		1.1710	0.4790		[14]
		1.1770	0.4820		[14]
		1.1820	0.4830		[14]
		1.1800	0.4830		[14]
		1.1840	0.4830		[14]
		1.1820	0.4840		[14]
	Mean	1.1760	0.4808		
	Minimal	1.1550	0.4776		
	Maximal	1.1840	0.4840		
Steel metallurgy plant		1.2226	0.4991		[8]
		1.2064	0.4953		[8]
		1.1944	0.4922		[8]
		1.1829	0.4886		[8]
		1.1786	0.4869		[8]
		1.1897	0.4904		[8]
	Mean	1.1958	0.4921		
	Minimal	1.1786	0.4869		
	Maximal	1.2226	0.4991		
Urban wastes		1.1540	0.4742	French southern cities/villages	[6]
		1.1620	0.4755	French southern cities/villages	[6]
		1.1552	0.4772	French southern cities/villages	[6]
		1.1543	0.4734	French southern cities/villages	[6]
		1.1673	0.4766	French southern cities/villages	[6]
		1.1600	0.4741	French southern cities/villages	[4]
		1.1609	0.4738	French southern cities/villages	[4]
		1.1600	0.4743	French southern cities/villages	[4]
		1.1613	0.4752	French southern cities/villages	[4]
		1.1547	0.4741	French southern cities/villages	[4]

		1.1585	0.4737	French southern cities/villages	[4]
		1.1476	0.4722	French southern cities/villages	[4]
		1.1494	0.4724	French southern cities/villages	[4]
		1.1479	0.4734	French southern cities/villages	[4]
		1.1578	0.4741	French southern cities/villages	[4]
		1.1577	0.4745	French southern cities/villages	[4]
	Mean	1.1587	0.4743		
	Minimal	1.1476	0.4722		
	Maximal	1.1673	0.4772		

Figure S1: (Left) Coal block found at station 3B during dredging operations (2014) where “Anzin 1912” was inscribed, illustrating its origin (Anzin, North of France) and period. Indeed, blocks of coal were stored and used by the French Navy for its fleets. Up to 400 tons of such blocks were discovered in the area, as it was used as a coal loading dock for French Navy fleet.
(Right) Lead plate from the "Magenta" French Navy battleship, sunk in 1876 in the entrance of Toulon Navy harbour.

Figure S2: Pb stable isotope ratios ($^{206}Pb/^{207}Pb$ and $^{206}Pb/^{208}Pb$, circle and square, respectively) and Pb content depth profiles (diamond) from 50-cm interface core collected at stations 3B and 23. The full and open symbols respectively represent total and HCl-extracted fractions. The filled areas with increasing grey scale indicate specific signature of industrial Pb, leaded gasoline and natural Pb, respectively. The full and dashed lines represent the variation range and the average value of the Pb isotopes ratios recorded in surface sediments (n = 54) of Toulon bay, respectively.

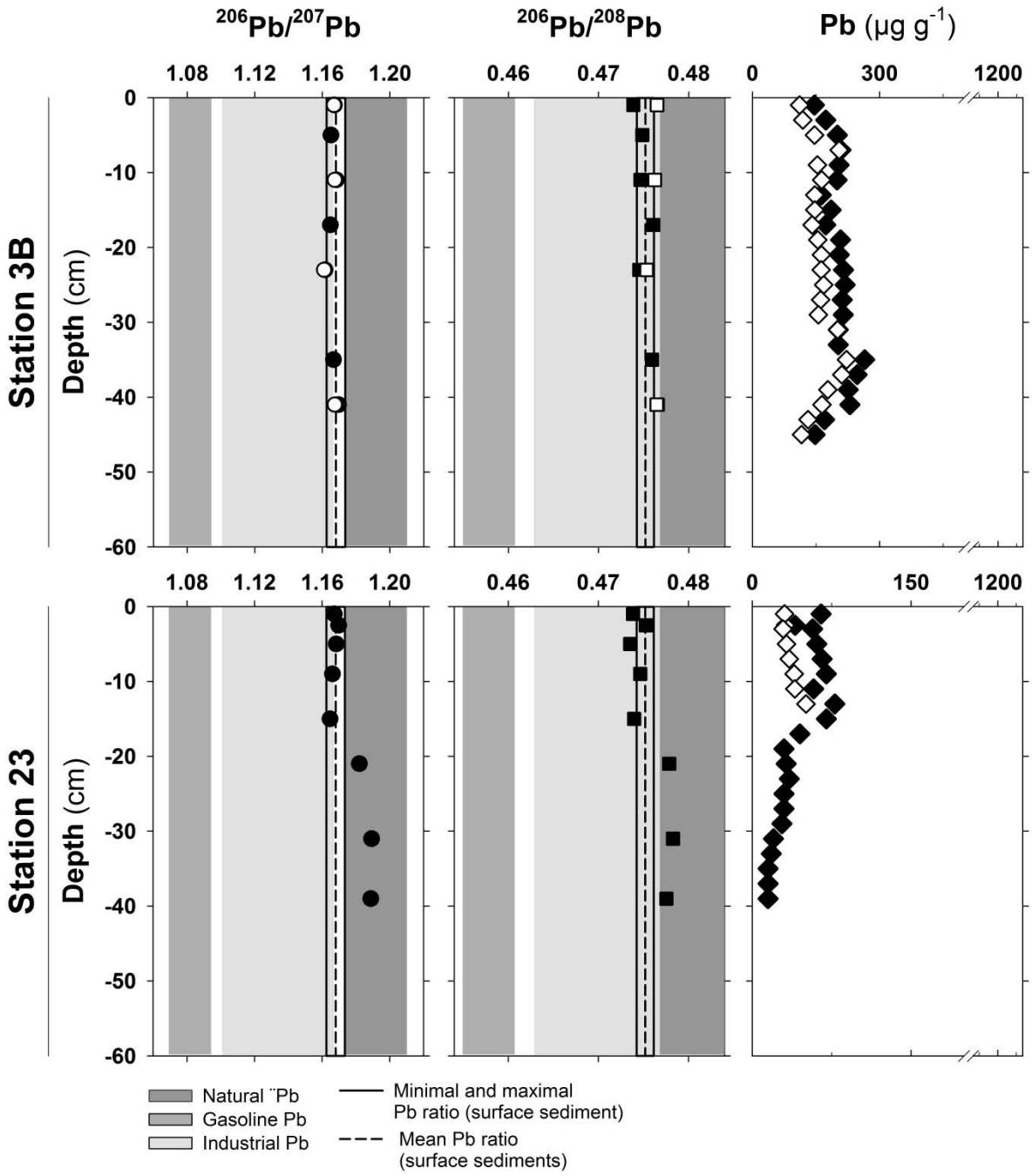

Figure S3: $^{206}Pb/^{208}Pb$ ratio as a function of $^{206}Pb/^{207}Pb$ for various Pb sources observed in the environment (Table A.1). Only the lines limiting the variation of Pb sources are shown in Figure 4 in comparison to samples from Toulon Bay.

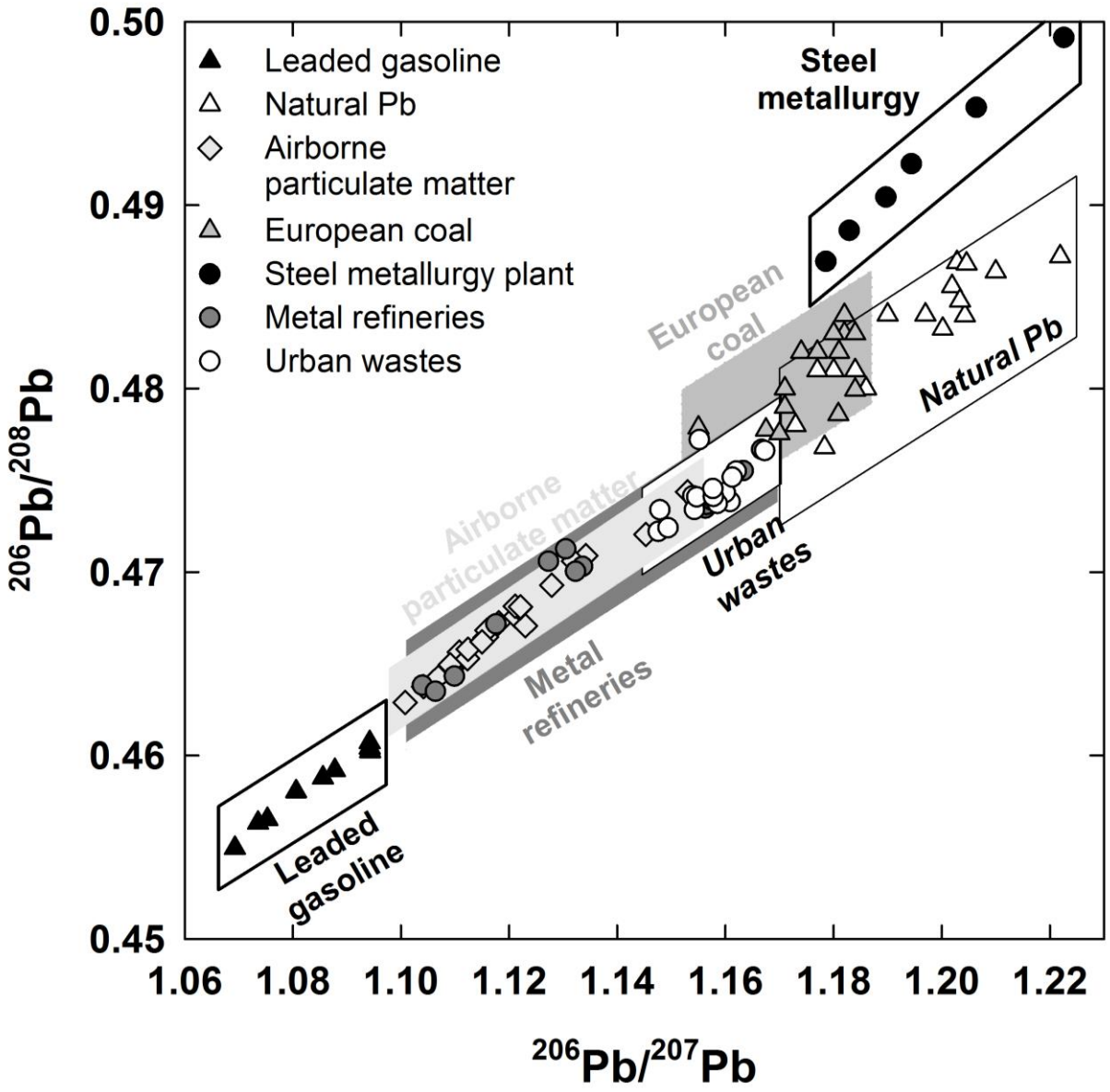

Figure S4: Time variation of pH, dissolved Pb, Fe and Mn concentrations released during sediment resuspension simulation using sediments from stations 3B and MIS (surface sediments, ~ $1g_{dw}$ L^{-1}). The open circles illustrate the initial values measured in seawater. The grey circles represent the contribution of porewater dilution and the black circles represent the measured values at 10 contact times.

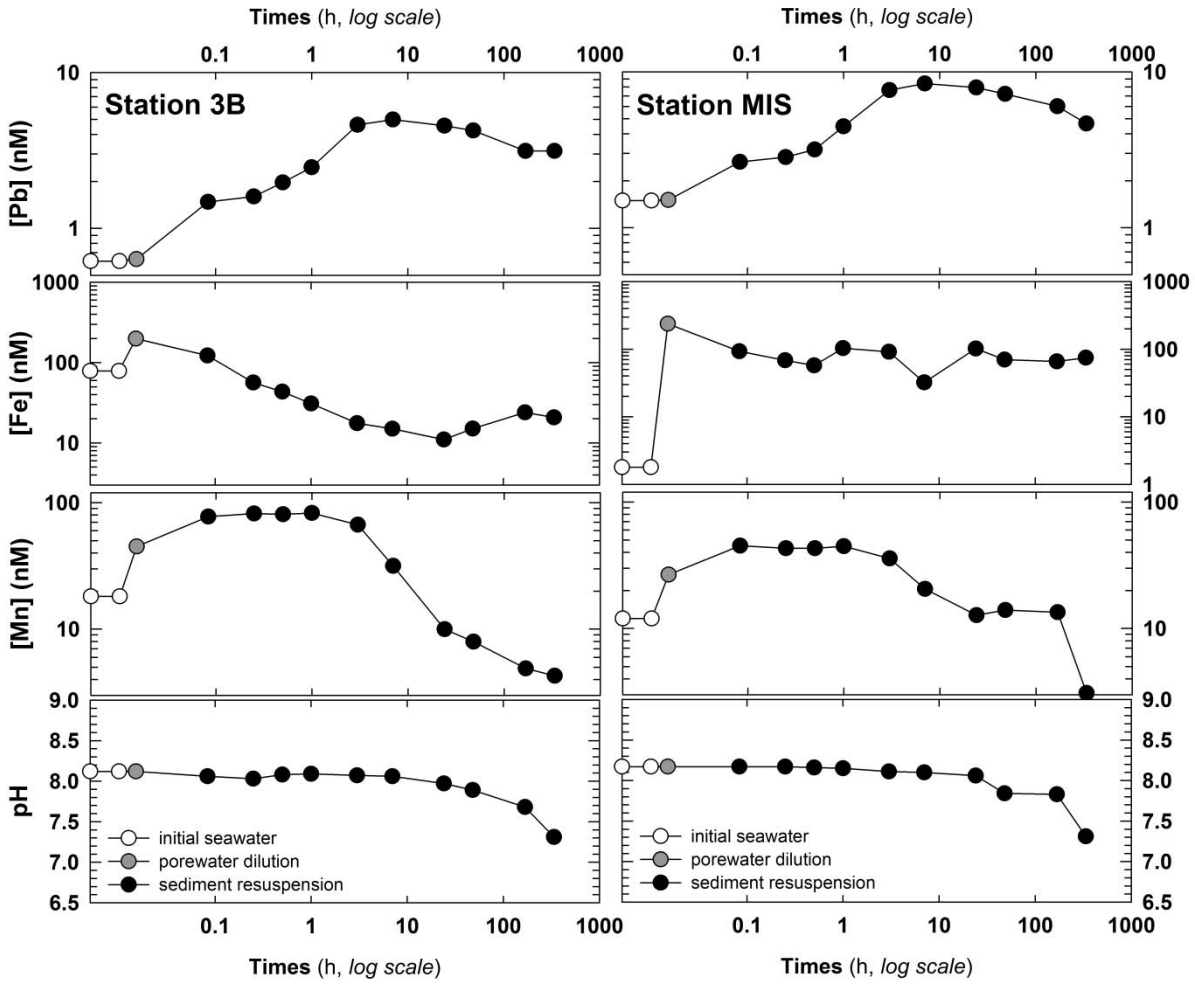

Figure S5: Assessment of the contribution of ^{anthropogenic}Pb source in Pb contamination of Toulon Bay's surface sediments (see text for more details).

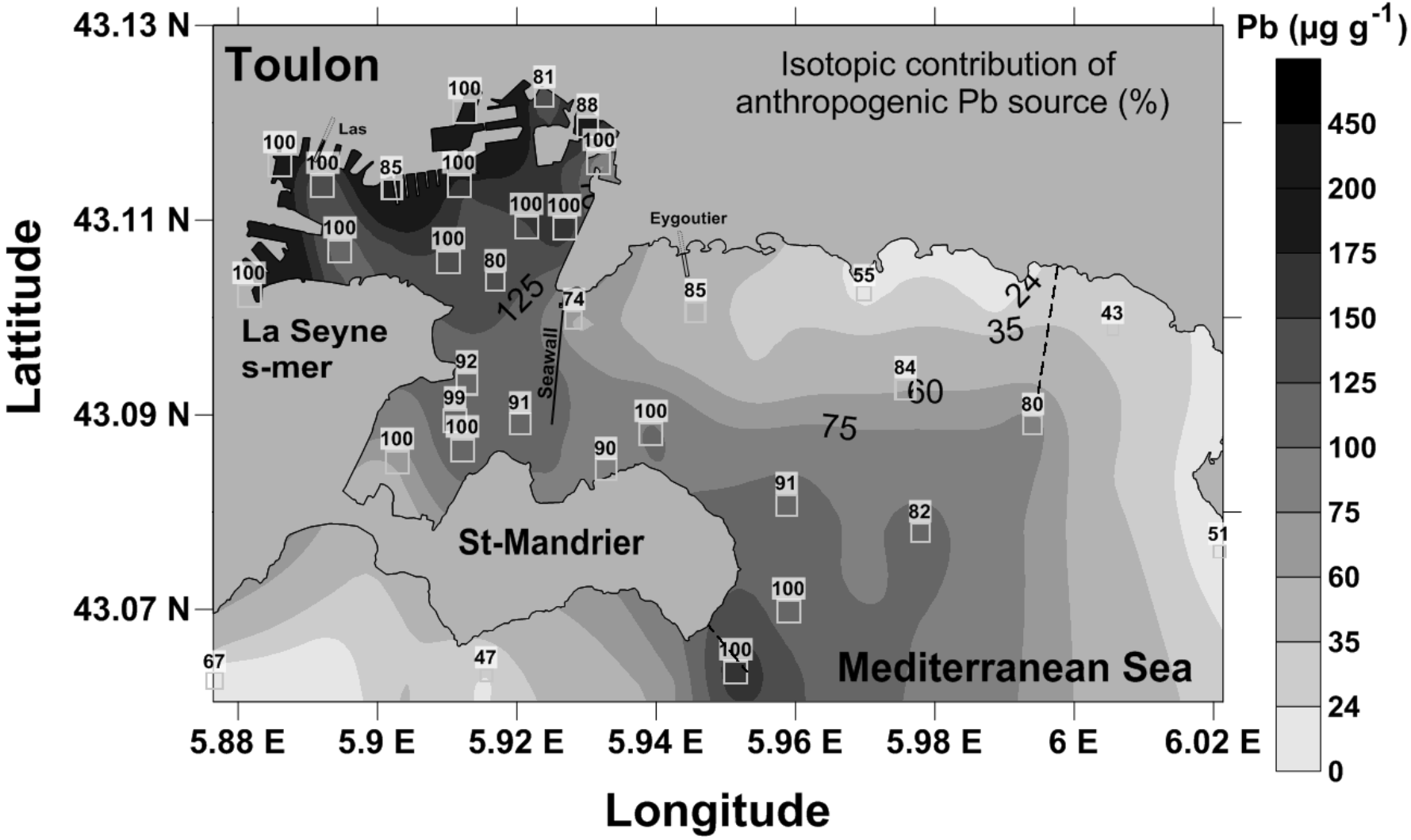

Figure S6: The relationship observed between the total and dissolved Pb at 40 stations around Toulon bay.

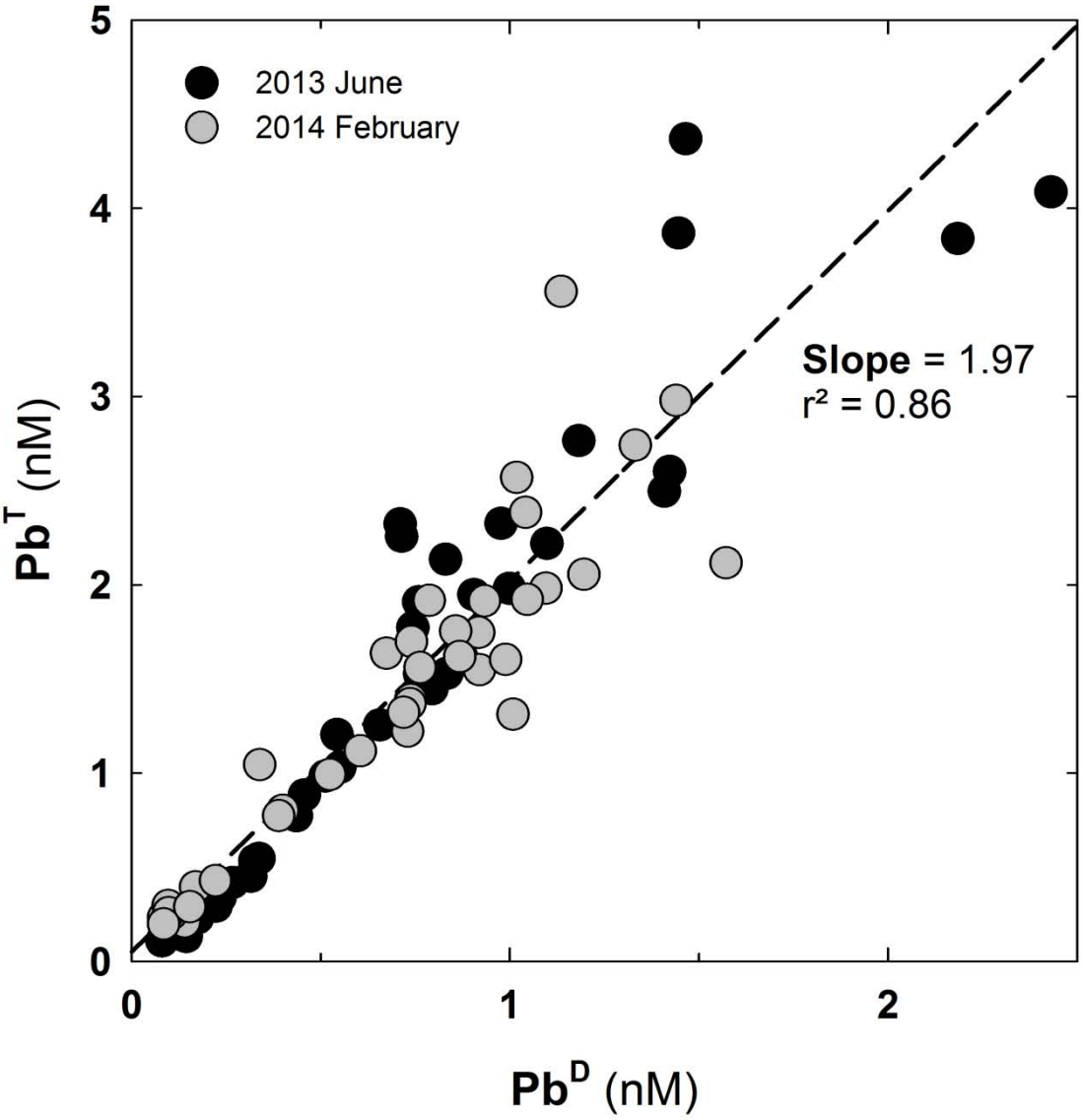

REFERENCES:

(1) Hamilton, E. I.; Clifton, R. J. Isotopic abundances of lead in estuarine sediments, Swansea Bay, Bristol Channel. *Estuar. Coast. Mar. Sci.* **1979**, *8*, 271–278.

(2) Monna, F.; Lancelot, J.; Croudace, I. W.; Cundy, A. B.; Lewis, J. T. Pb Isotopic Composition of Airborne Particulate Material from France and the Southern United Kingdom: Implications for Pb Pollution Sources in Urban Areas. *Environ. Sci. Technol.* **1997**, *31*, 2277–2286.

(3) Harlavan, Y.; Almogi-Labin, A.; Herut, B. Tracing natural and anthropogenic Pb in sediments along the Mediterranean Coast of Israel using Pb isotopes. *Environ. Sci. Technol.* **2010**, *44*, 6576–6582.

(4) Monna, F.; Othman, D. Ben; Luck, J. Pb isotopes and Pb, Zn and Cd concentrations in the rivers feeding a coastal pond (Thau, southern France): constraints on the origin (s) and flux (es) of metals. *Sci. Total Environ.* **1995**, *166*, 19–34.

(5) Chow, T. J.; Patterson, C. C. The occurrence and significance of lead isotopes in pelagic sediments. *Geochim. Cosmochim. Acta* **1962**, *26*, 263–308.

(6) Luck, J. M.; Othman, D. B. Geochemistry and water dynamics: II. Trace metals and Pb–Sr isotopes as tracers of water movements and erosion processes. *Chem. Geol.* **1998**, *150*, 263–282.

(7) Cloquet, C.; Carignan, J.; Libourel, G.; Sterckeman, T.; Perdrix, E. Tracing source pollution in soils using cadmium and lead isotopes. *Environ. Sci. Technol.* **2006**, *40*, 2525–2530.

(8) Véron, A.; Flament, P.; Bertho, M. Isotopic evidence of pollutant lead sources in Northwestern France. *Atmos. Environ.* **1999**, *33*, 3377–3388.

(9) Farmer, J.; Eades, L.; Graham, M. The lead content and isotopic composition of British coals and their implications for past and present releases of lead to the UK environment. *Environ. Geochem. Health* **1999**, *21*, 257–272.

(10) Chiaradia, M.; Cupelin, F. Behaviour of airborne lead and temporal variations of its source effects in Geneva (Switzerland): comparison of anthropogenic versus natural processes. *Atmos. Environ.* **2000**, *34*, 959–971.

(11) De Vleeschouwer, F.; Fagel, N.; Cheburkin, A.; Pazdur, A.; Sikorski, J.; Mattielli, N.; Renson, V.; Fialkiewicz, B.; Piotrowska, N.; Le Roux, G. Anthropogenic impacts in North Poland over the last 1300 years--a record of Pb, Zn, Cu, Ni and S in an ombrotrophic peat bog. *Sci. Total Environ.* **2009**, *407*, 5674–5684.

(12) Walraven, N.; Os, B. Van; Klaver, G. Trace element concentrations and stable lead isotopes in soils as tracers of lead pollution in Graft-De Rijp, the Netherlands. *J. Geochemical Explor.* **1997**, *59*, 47–58.

(13) D.az-Somoano, M. Stable lead isotope compositions in selected coals from around the world and implications for present day aerosol source tracing. *Environ. Sci. Technol.* **2009**, *43*, 1078–1085.

(14) Walraven, N.; van Gaans, P. F. M.; van der Veer, G.; van Os, B. J. H.; Klaver, G. T.; Vriend, S. P.; Middelburg, J. J.; Davies, G. R. Tracing diffuse anthropogenic Pb sources in rural soils by means of Pb isotope analysis. *Appl. Geochemistry* **2013**, *37*, 242–257.